REPORT DOCUMENTATION PAGE

Form Approved
OMB No. 0704-0188

The public reporting burden for this collection of information is estimated to average 1 hour per response, including the time for reviewing instructions, searching existing data sources, gathering and maintaining the data needed, and completing and reviewing the collection of information. Send comments regarding this burden estimate or any other aspect of this collection of information, including suggestions for reducing the burden, to Department of Defense, Washington Headquarters Services, Directorate for Information Operations and Reports (0704-0188), 1215 Jefferson Davis Highway, Suite 1204, Arlington, VA 22202-4302. Respondents should be aware that notwithstanding any other provision of law, no person shall be subject to any penalty for failing to comply with a collection of information if it does not display a currently valid OMB control number.
PLEASE DO NOT RETURN YOUR FORM TO THE ABOVE ADDRESS.

1. REPORT DATE *(DD-MM-YYYY)*	2. REPORT TYPE		3. DATES COVERED *(From - To)*
17/Jan/2002	THESIS		

4. TITLE AND SUBTITLE
THE PALEOCLIMATE OF THE DEAD SEA BASIN FROM THE LAST GLACIAL MAXIMUM TO THE HOLOCENE

5a. CONTRACT NUMBER

5b. GRANT NUMBER

5c. PROGRAM ELEMENT NUMBER

6. AUTHOR(S)
CAPT SWOVELAND THOMAS K

5d. PROJECT NUMBER

5e. TASK NUMBER

5f. WORK UNIT NUMBER

7. PERFORMING ORGANIZATION NAME(S) AND ADDRESS(ES)
ARIZONA STATE UNIVERSITY

8. PERFORMING ORGANIZATION REPORT NUMBER
CI02-7

9. SPONSORING/MONITORING AGENCY NAME(S) AND ADDRESS(ES)
THE DEPARTMENT OF THE AIR FORCE
AFIT/CIA, BLDG 125
2950 P STREET
WPAFB OH 45433

10. SPONSOR/MONITOR'S ACRONYM(S)

11. SPONSOR/MONITOR'S REPORT NUMBER(S)

12. DISTRIBUTION/AVAILABILITY STATEMENT
Unlimited distribution
In Accordance With AFI 35-205/AFIT Sup 1

DISTRIBUTION STATEMENT A:
Approved for Public Release -
Distribution Unlimited

13. SUPPLEMENTARY NOTES

14. ABSTRACT

20020204 091

15. SUBJECT TERMS

16. SECURITY CLASSIFICATION OF:			17. LIMITATION OF ABSTRACT	18. NUMBER OF PAGES	19a. NAME OF RESPONSIBLE PERSON
a. REPORT	b. ABSTRACT	c. THIS PAGE		75	19b. TELEPHONE NUMBER *(Include area code)*

Standard Form 298 (Rev. 8/98)
Prescribed by ANSI Std. Z39.18

THE PALEOCLIMATE OF THE DEAD SEA BASIN

FROM THE LAST GLACIAL MAXIMUM TO THE HOLOCENE

by

Thomas K. Swoveland

A Thesis Presented in Partial Fulfillment
of the Requirements for the Degree
Master of Arts

ARIZONA STATE UNIVERSITY

December 2001

THE PALEOCLIMATE OF THE DEAD SEA BASIN

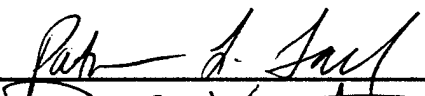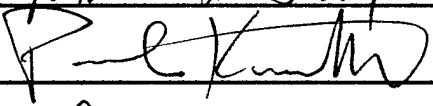# FROM THE LAST GLACIAL MAXIMUM TO THE HOLOCENE

by
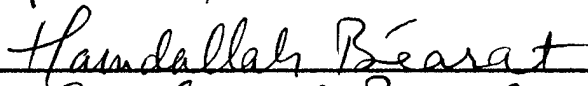
Thomas K. Swoveland

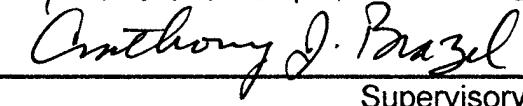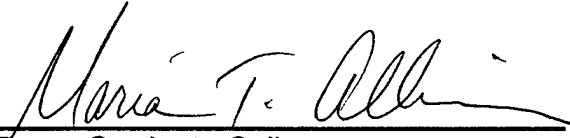has been approved

November 2001

APPROVED:

_____ , Chair

_____

_____

Hamdallah Béarat

Anthony J. Brazel
_____
Supervisory Committee

ACCEPTED:

_____
Department Chair

_____
Dean, Graduate College

ABSTRACT

The purpose of this study was to determine the late glacial paleoclimate of the Southern Levant. A study of $\delta^{13}C$ and $\delta^{18}O$ in carbonates (aragonite) was undertaken from a Lisan Core 3, a laminated core, collected from the Lisan Peninsula in the Dead Sea. Accelerator Mass Spectrometer (AMS) ages demonstrated that the core spanned the period from the Last Glacial Maximum (LGM) to the Holocene (20-12 thousand years ago (kya)). Results derived from carbon and oxygen isotopes provide insight into the paleoclimate of the Southern Levant. The period from 20-14.6 kya was dry and cool, with little organic matter being washed into the Dead Sea Basin. This interpretation is based on higher isotopic values ($\delta^{13}C$ values as high as 1.57) than are found in the modern Jordan River, which has $\delta^{13}C$ values of −7.2. During the interval from 14.2-12.5 kya, values for $\delta^{13}C$ and $\delta^{18}O$ were much more dilute, with $\delta^{13}C$ values as low as −14. This dilution demonstrates increased precipitation and/or flooding events that washed organic matter into the basin. The results of this study agree with other studies based on paleolake levels, pollen levels and paleoclimate studies from the Dead Sea Basin.

ACKNOWLEDGMENTS

TABLE OF CONTENTS

LIST OF TABLES

LIST OF FIGURES

INTRODUCTION

Project Background

This research supports a multidisciplinary project under the direction of Dr. Philip Edwards, Department of Archaeology, La Trobe University, Melbourne, and Drs. Patricia Fall and Steven Falconer, Departments of Geography and Anthropology, Arizona State University, Tempe, Arizona. This larger study focuses on investigating long-term paleoenvironments and human ecology on the Dead Sea Plain, Jordan over the last 15,000 years. Specific objectives of this project are to interpret the relationship between agricultural intensification and its environmental impacts along the Jordan rift valley.

As part of this larger project the goal of the study presented here is to reconstruct the paleoclimate of the Dead Sea Basin during the period from 20-12.4 kya (thousands of years ago). Paleoclimatic conditions would have greatly affected the migration and settlement patterns of humans in this region.

Understanding the paleoclimate of the Dead Sea basin provides useful information into the ability of early settlements to survive and/or flourish. Numerous studies have been performed on the climate of the Holocene (Avner, 1990; Frumkin et al., 1991; McCreery, 1980; Rast and Schaub 1974, 1978, 1980, and 1981) and its effects on Bronze Age settlements, whereas the paleoclimate of the period from the Late Glacial Maximum (LGM) to the Holocene is in dispute.

One group of researchers concluded numerous gypsum ($CaSO_4$) varves represent the driest period, extending from 23-22 to 16-15 kya BP (Huckriede and Wiesemann, 1968; Goodfriend and Magaritz, 1988; Abed and Yaghan, 2000) indicating the glacial maximum in the Near East was cool and dry. However, others have inferred pluvial conditions during the period from 25 kya to 10 kya based upon marl deposits and gamma-ray log analysis (Horowitz, 1979, 1992; Bowman, 1990; Neev and Emery 1967, 1995).

By determining the effective precipitation, temperature and lake levels of the Dead Sea basin this study hopes to provide critical insight into the past environments of the Dead Sea Basin and to support the above mentioned multidisciplinary study.

Tectonic Setting

The Dead Sea occupies a remnant of the area of its Pleistocene predecessor, Lake Lisan, which existed from 70–10 kya before present (Figures 1 and 2). It is hypothesized that lake Lisan underwent two distinct periods of geomorphic and hydrological evolution. The first was a result of an increased supply of freshwater, which caused the lake levels to increase, the formation of a density layer structure, and the precipitation of aragonite. The second evolution resulted from reduced freshwater input, causing the lake level to lower, mixing (or complete overturning of its water), and the precipitation of gypsum (Starinsky et. al, 1997). The late Pleistocene-Holocene timeframe was marked by dramatic

climatic fluctuations, which are reflected in the advance and retreat of the global ice sheets, changes in sea level and shifts in climatic zones (Broeker, and Denton, 1989). Thus, these distinctly different evolutionary developments of the Dead Sea were the result of very different climatic environments. Evidence of this climatic variation reveals itself through analysis of the precipitated sediments in the Lisan Formation (Neev and Emery, 1967).

What is less clearly understood is how these climate changes may have affected the early civilizations of the Near East. Rifting and active tectonics within the Jordan Valley created the landscape that originally led people to this area. The down-dropped graben in which the Dead Sea formed, also caused the formation of the Jordan River. This was a major source of freshwater for the area, flowing southward through the Jordan Valley, allowing early civilizations to prosper.
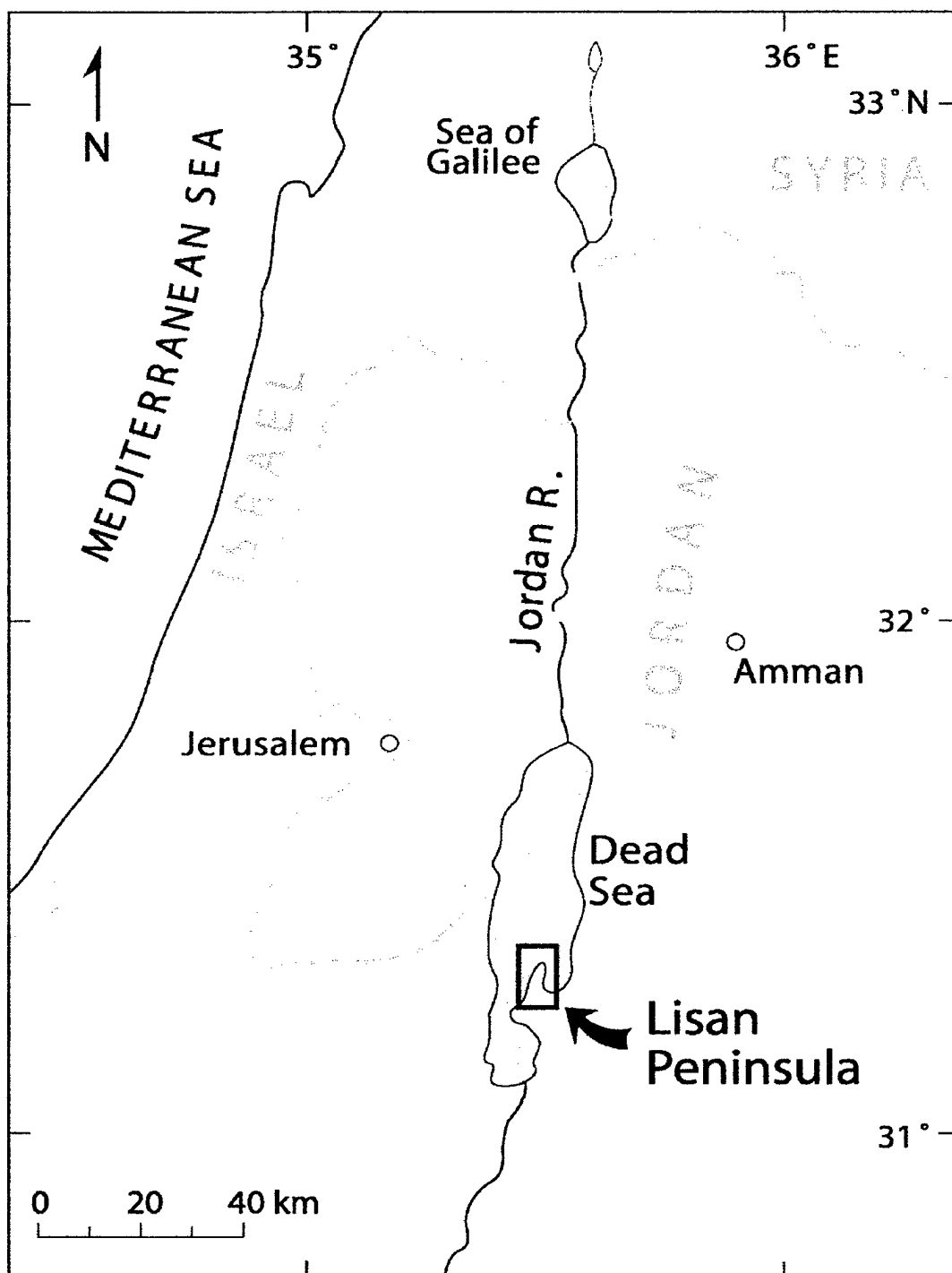
Fig 1. Map location of the Dead Sea in the Jordanian Rift (by B. Trapido-Lurie).
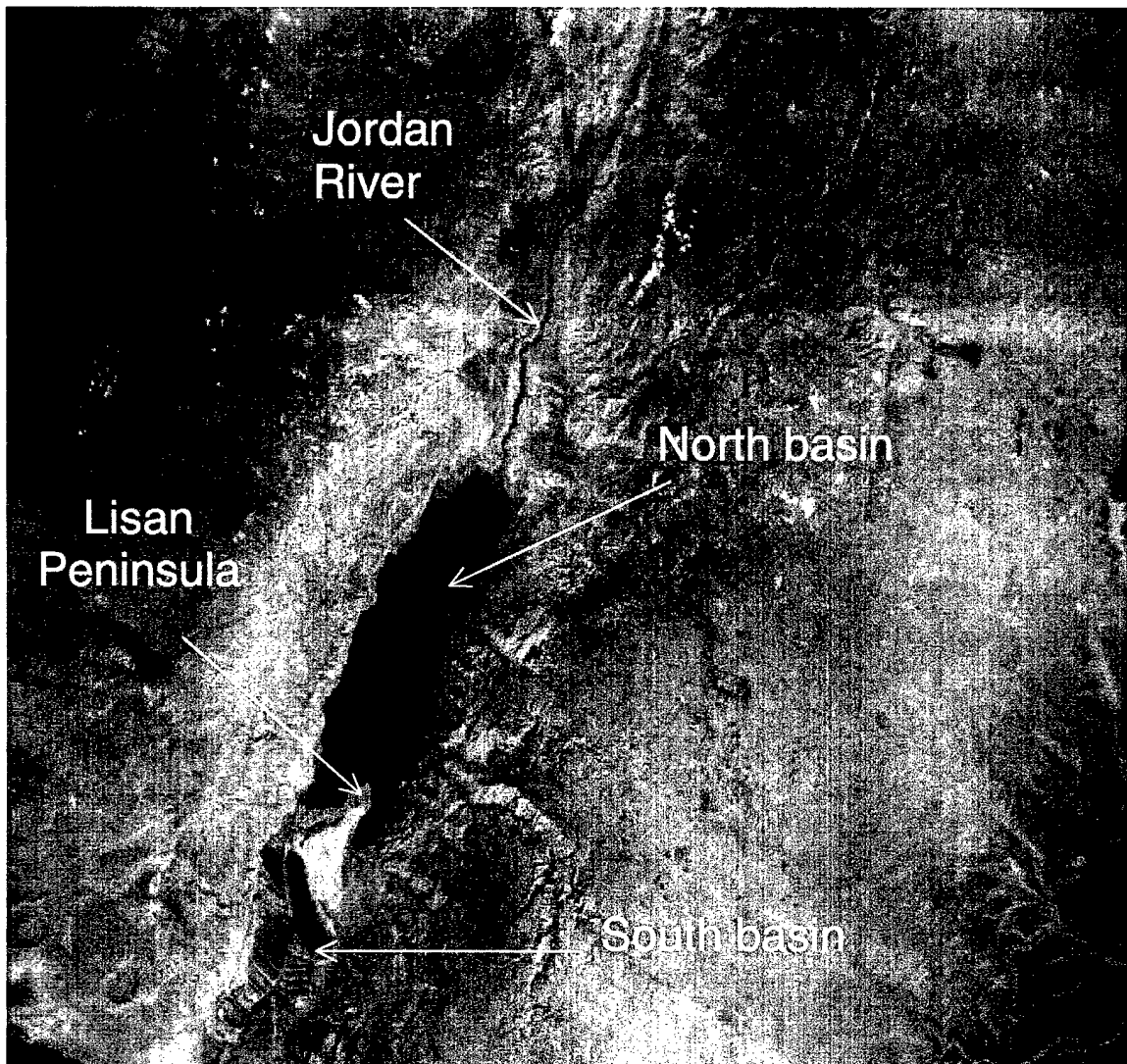
Fig 2. Satellite view of Dead Sea Basin showing location of Lisan Peninsula.

Tectonic activity also produced many springs along the rift, particularly along the east side. Strong tectonic activity has been documented in and around the Dead Sea area since Biblical times. Historical literature describes earthquakes that could have exceeded magnitude 7 in the years 1202, 1546, 1759 and 1837 (Arieh 1967). The Hula Valley at the northern end of the rift is the center for most major seismic events. The Hula Valley is an expanding valley between the Dead Sea Fault, the Jordan and Rachaya fault and the Yammuneh fault, with the youngest portion of this system being the Azaz fault (Garfunkel, 1981). The eastern boundary of this zone forms a complex pattern, and displays considerable evidence of the westward movement of tectonic activity during the Pleistocene (Heimann *et, al.*,1990).

Geochemistry of the Dead Sea

A myriad of studies are influential to the understanding of the Dead Sea's dynamic environment. Katz and Kolodny (1977) researched the geochemical evolution of the Dead Sea basin through salinity, depth, chemical and stable isotope composition. They concluded Lake Lisan was half as saline as the modern Dead Sea. Lake Lisan evolved from a hypersaline lake to a fresher water lake due to influx of fresh water from the Jordan River, which they demonstrate through Sr/Ca ratios in aragonite (Katz and Kolodny, 1977). Their model required a lake depth of at least 400m and more likely 600m. This leads to an important assumption, that the tectonic opening of the deep Dead Sea

basin predated the deposition of the Lisan Formation. Katz and Kolodny (1977) go on to describe aragonite precipitation to be salinity dependent, and nearly temperature independent, therefore, mineral precipitation occurred after freshwater from the Jordan River entered the basin. The salinity gradually increased to the point where aragonite was able to precipitate, normally occurring in the summer months. They determined the dilution necessary to precipitate aragonite was 1:3, one-part Lake Lisan waters to three parts freshwater. This was possible due to the stratified nature of the basin.

Stiller *et al.* (1985) studied the enrichment of carbon-isotopes in evaporating brines within the Dead Sea, focusing on the possible cause of extreme $\delta^{13}C$ enrichment (in excess of +14 per mil). Their study found no methane production, indicating a totally inorganic enrichment of ^{13}C, and showing how increasing density (salinity) occurred as pH and ΣCO_2 decreased. This proved to be an important point. Evaporation related to the loss of CO_2 from the brines is responsible for ^{13}C enrichment (Stiller *et al*, 1985). This point supports the work of Katz and Kolodny (1977) that decreasing pH (or increasing salinity) is correlated with enrichment with ^{13}C.

Luz *et al.* (1997) enhanced Stiller's (1985) work with a second study titled *Carbon Dynamics in the Dead Sea.* By introducing the possibility of organic carbon influx into the Dead Sea as a cause for ^{13}C depletion, the authors provided an isotopic mass balance equation from which the addition of organic carbon can be determined.

$$\delta^{13}C = x\delta^{13}C_{org} + (1-x)\delta^{13}C_o$$

In this equation, x is the added mole fraction of organic carbon ($^{13}C_{org}$), and $^{13}C_o$ is the isotopic composition before the addition.

The authors found the total carbon (TC) in the Dead Sea has been previously overestimated due to the high borate content within the Dead Sea. In addition, evidence of significant seasonal $\delta^{13}C$ fluctuations were evident during holomictic years as well as evidence of increased quantities of TC as a result of massive rains and floods.

In a more recent study, Barkan et al. (2001) investigated the carbon dioxide cycle within the Dead Sea in an attempt to determine when the major aragonite precipitation events would occur. Most researchers to this point believed aragonite precipitation occurred during the hyperarid summer months when the Dead Sea reached saturation with respect to Ca. Neev and Emery (1967) had observed whitting events during a summer research cruise which was the result of the precipitation of aragonite in the surface waters of the Dead Sea. However, Barkan et al. (2001) demonstrated thermodynamically that the majority of aragonite was likely precipitated during winter months when Dead Sea brine with a high Ca content mixed with 90% freshwater runoff with a high-bicarbonate content. The authors further stated that in the late Pleistocene inorganic carbonate precipitated by the mixing of two solutions, Ca^{2+} and HCO_3^- (the formation of aragonite) was six times as prevalent as it is today. Therefore, they

effect of the Younger Dryas, a dramatic cooling event that occurred during the last deglaciation around 11-10 kya.

Horowitz (1979) described climate phases within the Southern Levant. He stated a glacial phase began about 70-65 kya and terminated approximately 11 kya. Several pluvial phases were associated with this period that lasted through 45 kya. During this period, Mousterian people settled through the Negev and Sinai. The first interstadial period occurred between 45 kya and 35-32 kya, and signified a very dry climate that resulted in low settlement levels. The second pluvial phase occurred between 43 kya and 22-20 kya. During this period Upper Paleolithic people settled the land again through the Negev and Sinai. A second interstadial period occurred between 22-20 kya and 18-16 kya. The third pluvial phase occurred 18 kya through 12 or 11 kya with this period dominated by Epipaleolithic settlements. A dramatically arid phase occurred globally at approximately 21-15 kya.

Southwest Indian Monsoon Effects on the Paleoclimate of the Levant

The paleoclimate of the Dead Sea basin from the LGM to the Holocene can be characterized as being pluvial or interpluvial. Campo (1986) utilized marine pollen and foraminifera to develop a 20,000-year representation of the Indian continental vegetation and Indian monsoon during the late Quaternary.

Campo (1986) developed three main points regarding the paleoclimate off Southwest India.

1. The LGM was very arid, suggested by the absence of mangrove vegetation that was a result of a very weak southwesterly monsoon flux, causing a reduced summer rainfall.

2. The summer monsoon reestablished itself diachronically north to south after the northward migration of the Intertropical Convergence Zone just after the LGM. The strongest summer monsoon rains over southwest India occurred at 11 kya.

3. The strongest summer monsoon rainfall occurred concurrently with the maximum summer insolation of the Northern Hemisphere at 11 kya, emphasizing the role of solar radiations at lower latitudes.

This monsoonal study further supports the climatological and geochemical work within the Southern Levant to interpret the timing of pluvial and interpluvial phases.

Problem Statement

The focus of this study was to determine the paleoclimate of Dead Sea basin for the period 20-12 kya by analyzing a 12.25m core (Lisan Core 3) taken from the Lisan Peninsula at the southern edge of the northern basin of the Dead

Sea.   Stable isotopes, mineralogical and elemental analyses were used to interpret the geochemistry and hydrology of the Dead Sea and to interpret past changes in precipitation.

STUDY AREA

The Southern Levant is an active tectonic region. Tectonic activity formed the Dead Sea Basin and helped shape the geomorphology of the region. Today the Dead Sea Basin lies in a hyperarid desert that receives the majority of its freshwater from the Jordan River to the north, although springs and winter runoff events provide some freshwater influx. Vegetation is very sparse in the Dead Sea basin, but becomes denser as elevation increases.

Tectonics

The Dead Sea Basin (31°30' N, 35° 25' E) is a depression along the Dead Sea Rift (a transform fault). This rift is an intracontinental plate boundary that began during the late-Cenozoic breakup of the previously continuous Arabo-African continent (Garfunkel, 1993). The continental crust of the region was first consolidated during the Pan-African orogeny of the Late Proterozoic, and then this area became stable during most of the Phanerozoic (Garfunkel, 1988). This period of stability was interrupted by the formation of the Mediterranean Sea during the Permian to early Mesozoic by rifting. This activity also formed the strongly faulted belt, 70-100 km wide, inland of the current Sinai-Israel coast that became the Dead Sea Rift (Ginzburg and Folkman, 1980). The Cenozoic continental breakup produced numerous rifts and led to the splitting of the Arabian plate from the African plate with the Dead Sea rift forming a part of this

new boundary of the Arabian plate (Garfunkel, 1993). The Dead Sea Basin itself is considered a pull-apart basin caused by left-lateral faults (the Jericho and Arava strike-slip faults) that are delineated by normal faults (Garfunkel, 1993). The average slip rate of this transform fault has been calculated to be about 5-10 mm/yr (Garfunkel, 1993).

The Dead Sea Basin appears to be the most active tectonic section along the Dead Sea-Jordan rift system (Shapira, 1993). Documented evidence of strong seismic activity has been recorded through history. In the past 1,000 years six earthquakes with an estimated maximum magnitude of at least 5.8 have been recorded or interpreted (Shapira, 1993). Historical literature describes earthquakes that could have exceeded magnitude 7 in the years, 1202, 1546, 1759 and 1837 (Arieh 1967).

The Lisan Peninsula, which divides the northern and the southern basins of the Dead Sea (see Fig 2), has been uplifted due to buoyancy created by a salt diapir directly under the peninsula. This diapir has been estimated to extend to a depth of 4.5-5 km (Abu Ajamieh et al., 1989). The tectonic importance of the Dead Sea Basin cannot be overstated given the formation of a large portion of the substrata resulted from tectonic action.

Geomorphology/Topography

The Dead Sea is a terminal lake that receives the majority of its freshwater from the Jordan River, which empties into the northern portion of the basin. The Jordan River drains an area some 2,730 km^2 from the Golan Heights and mountains of southern Lebanon (Bowman, 1993). The Dead Sea occupies the lowest point on earth, at 404m below mean sea level. Normal fault escarpments rise steeply to the west and east of the basin forming a well-defined graben. These steeply rising escarpments provide an ideal environment for the formation of alluvial fans, gorges, canyons and springs reflecting past seismic events. Bowman (1993) describes several alluvial fans present on the western slope of the Dead Sea Basin to have been originally deposited below lake level. The aridity of the Dead Sea basin coupled with entrenchment of the sedimentlogical structures by fluvial processes makes the Dead Sea Basin an ideal location to study desert geomorphology.

Climate

The Dead Sea Basin is a hyperarid region with a mean annual precipitation of 50 mm or less (Bowman, 1993). Summer temperatures routinely reach 30-40°C with a mean of 15°C in January. Surface soil temperatures may reach over 50°C in the summer (Bowman, 1993). Annual potential evaporation is

over 2 m, and the mean annual humidity is 45-50% (Survey of Israel, 1995). The winter represents the rainy season with year-to-year variability quite high. Wet winters can double the annual precipitation (50 mm average annual precipitation) with extremely dry winters providing no precipitation. The drainage basins have an altitude of 800-1,000 m on the western escarpment and 2,100 m on the eastern escarpment of the Dead Sea with an annual precipitation greater than 600 mm/yr. This can cause great flooding to the basin (Bowman, 1993).

Hydrology

The Dead Sea water column is composed mainly of two water bodies: a deep water, comprising the majority of the basin's volume, and a shallow upper layer only a few meters thick. This water column depends primarily on factors such as season, freshwater input and salinity. The maximum depth of the Dead Sea is 324 m, and represents the deepest terrestrial spot on earth (Anati, 1993). The Dead Sea is saturated with respect to aragonite, halite and gypsum, and precipitates salts mostly around the shores of the lake, with some salt precipitation occurring in the interior (Anati, 1993).

The Jordan River flows south and brings freshwater into the northern portion of the Dead Sea Basin. Small amounts of freshwater also enter into the basin through fluvial process on the eastern side of the basin. Being a terminal lake, the Dead Sea is a hypersaline water body that is recharged by precipitation,

flood events and river input. Bicarbonate and calcium is supplied to the Dead Sea from the Jordan River where it mixes with CO_2 in the Dead Sea to form carbonate minerals. Salts are also washed into the basin and become supersaturated during drying events and precipitate mainly along the shores. Sulfur production is thought to occur during flood events when a freshwater interface over the hypersaline water body allows biotic activity to occur. This biotic activity possibly reduces sulfates and sulfides present in the water into native sulfur. Neev and Emery (1995) postulated that whenever the Dead Sea fell below the critical level of –400 m msl, halite become the major mineral phase precipitating within the Dead Sea. Currently the Dead Sea is below this level and observations indicate halite is indeed precipitating along the shoreline. Paleolake levels have dipped below –400 m msl in the past. It has been hypothesized the Dead Sea reached below –700 m msl during the Late Pleistocene/Holocene transition (Niemi, 1997).

Modern lake levels have also decreased dramatically with the introduction of commercial potash production in the southern basin, and diversion of the Jordan River's freshwater for agriculture. Since 1932 the level of the Dead Sea has dropped from –391 m msl to –395 m msl in 1936, and again to almost –398m msl between 1955 and 1964 (Neev and Emery, 1995). In 1988 it dropped to –408 m msl (Steinhorn and Assaf, 1980; Klein, 1986; Anati and Stiller, 1991-all based upon measurements by the Dead Sea Works).

Vegetation

The environment of the Dead Sea Basin is Saharo-Sindian, which is defined by its very low precipitation and mild winter. Frequently the entire amount of annual precipitation can occur within a several hour winter rainfall (Horowitz, 1979). Rates of evaporation can be up to a hundred times greater than rates of precipitation. Soils are immature, such as hamades (barren desert surface composed of consolidated material), sands and sebkhas (smooth, flat plain usually high in salt; after a rain the plain may become a marsh). Plants and animal diversity is rather restricted, but show considerable adaptation to the desert environment (Horowitz, 1979). Plants have a quick growth rate and produce drought resistant seeds that can survive several years before germinating when wetted. Near the Dead Sea where soils are gypsiferous, plants such as *Suaeda asphaltica* and *Chenolea arabica* are common (Horowitz, 1979). Springs and wadi beds create microenvironments with more vegetation.

METHODS

Several factors were considered in this study:

1. Type of sample media-For this study sediment cores were collected using a Livingston piston corer.

2. Depositional characteristics of the sampled sediment-Would the sediment be deposited in varves or as massive, slumped marl-like substances reworked by wind, wave or other physical action?

3. An accurate dating method to determine the study's duration-Radiocarbon was chosen for its accuracy, speed and availability.

4. Which analytical methods would provide the most usable information-Powder XRD was chosen to determine mineral phase due to its availability at Arizona State University, its accuracy, ease of use and relative low cost. PIXE was chosen to determine sulfur content in the mineral due again to its availability, ease of use and relative low cost. Sulfur (as opposed to Calcium or Magnesium) percent was chosen because sulfur percent could be used to indicate hypersalinity. Stable isotopes of carbon and oxygen were chosen due to the availability of a stable isotope lab at Arizona State University, and their well-known ability to determine climate signals from lake sediments.

Field Methods

Eight sediment cores from four locations [(1) Dead Sea Cores 1-3; (2) Lisan Cores 1-3; (3) Lisan Core 4 and (4) Lisan Core 6)] were collected from the western and northernmost flank of the Lisan Peninsula in January-February 2000. Dead Sea Cores 1-3 and the section of Lisan Core 3 used on this study (668-1225cm) were collected with a hand operated 5cm diameter Livingston piston corer (Fig. 3). A truck mounted Witte drill rig (14cm diameter corer) operated by the National Resource Authority of Jordan was used to collect Lisan Cores 1, 2, 4, 6 and the upper 5m of Lisan Core 3. Sediment cores were labeled, wrapped in plastic wrap and aluminum foil in the field. Cores were shipped in wooden core boxes from Jordan to the ASU Department of Geography's paleoecology lab where they were analyzed.

Sediment Cores

This study focuses on Lisan Core 3 from 691-1,225 cm. This core was chosen for analyses because it represents the least disturbed and most continuously laminated sediments recovered from the Lisan Peninsula.
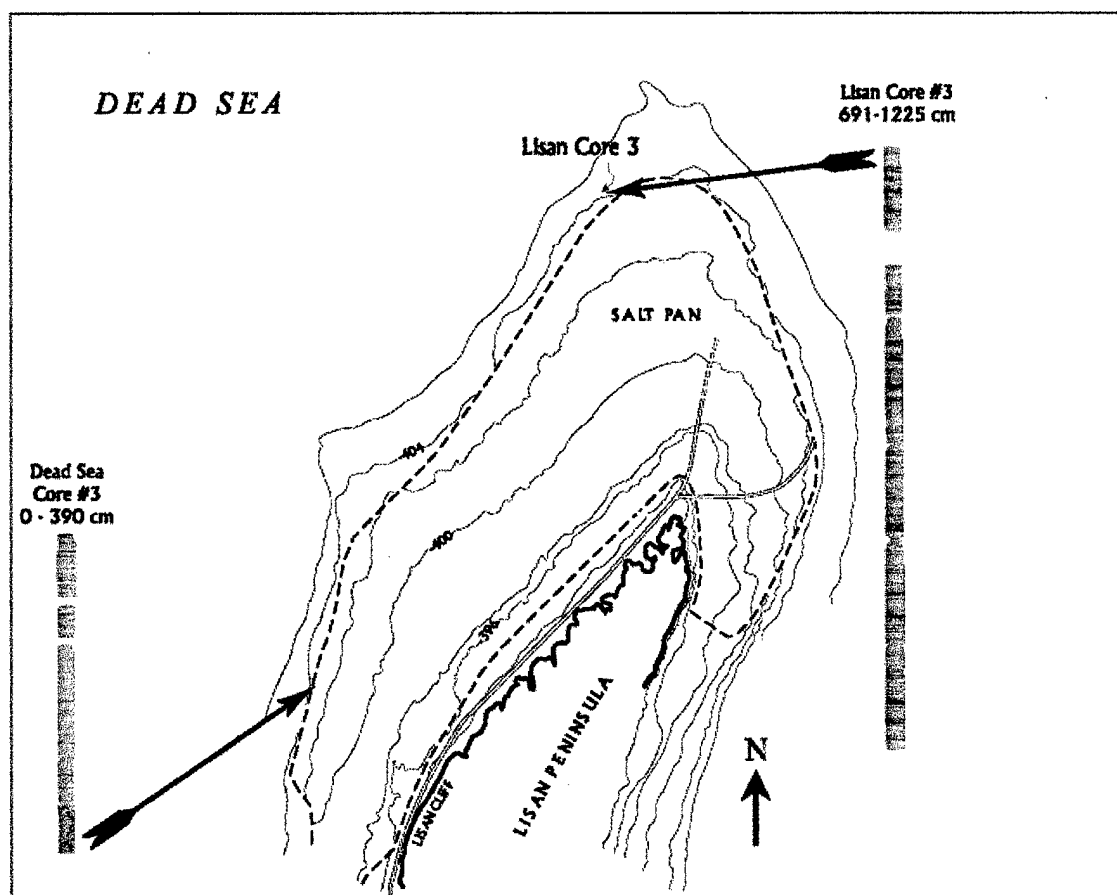
Fig 3. Map of northern end of the Lisan Peninsula showing locations of cores used in this study.

In addition, three carbonate samples from the upper deposits of Dead Sea Core 3 were used for comparison with Lisan Core 3. Core sections were cut into two halves lengthwise to observe depositional varves. Each core was then photographed with a high-resolution digital camera in 15 cm long overlapping images. This produced an electronic image gallery of each core sequence (Fig. 4).

Sediment cores were comprised of laminated sediments consisting of alternating white carbonate and dark gray-green detrital laminae (Fig. 5). White (carbonate) laminae were sampled from the cores approximately every 15 cm, depending upon the location of the individual carbonate lamina. Once the layers were exposed, careful scraping with a surgical scalpel removed each specific lamina to be sampled. Care was taken not to contaminate the samples with material from the adjacent detrital lamina. Sample material was then placed into glass vials, labeled, and desiccated in an oven at 65°C for ten hours.

Analytical Techniques

Accelerator Mass Spectrometry (AMS) Analyses

In order to determine the age of the sediments, five wood macrofossils imbedded in the sediments were recovered (three from Lisan Core 3, and two from Dead Sea Core 3). The wood macrofossil samples were sent to Beta Analytical, Inc. for AMS analyses. The sedimentation rate for Lisan Core 3 was
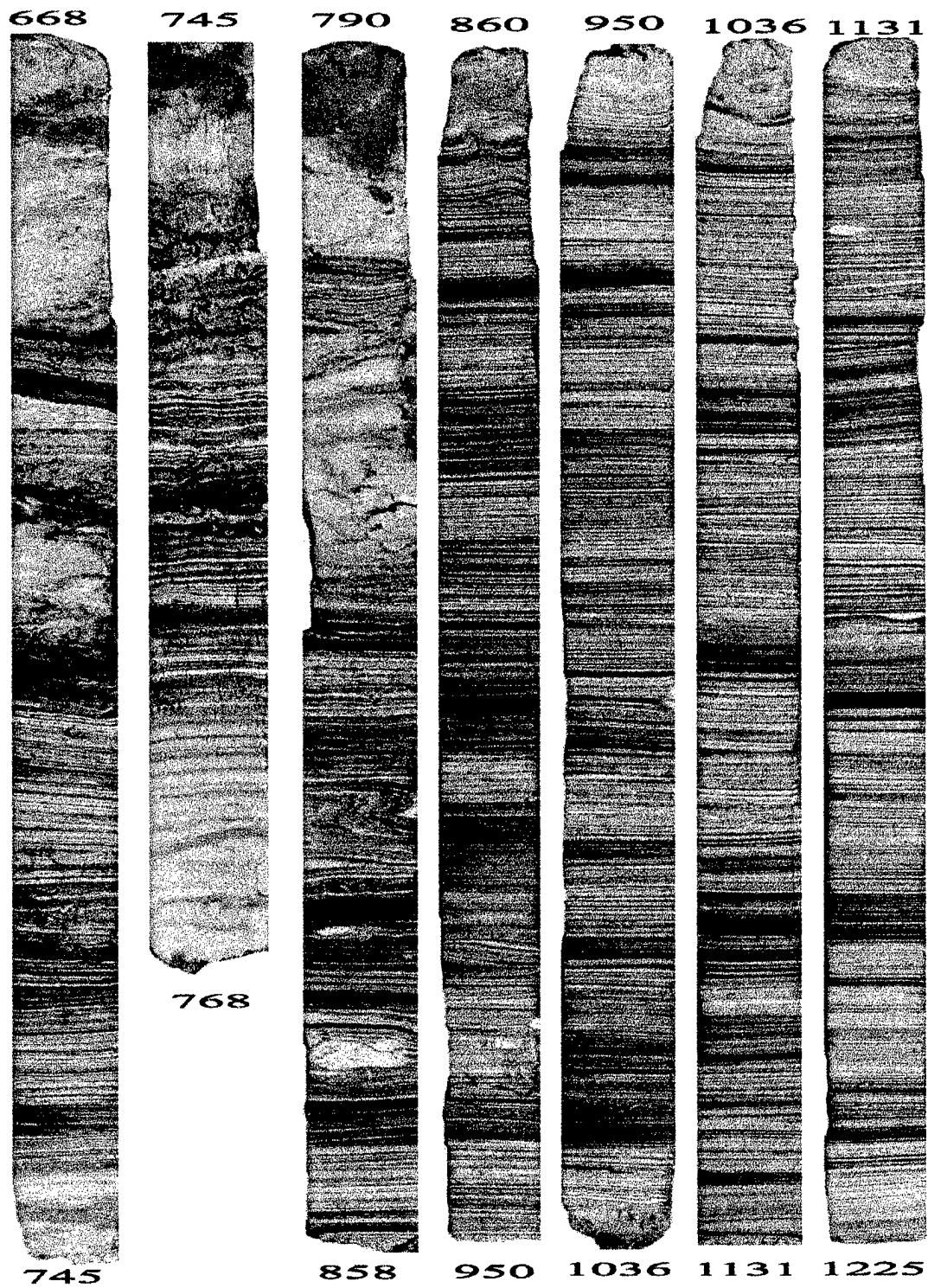
Fig 4. Detailed image of Lisan Core 3 (668-1225cm).
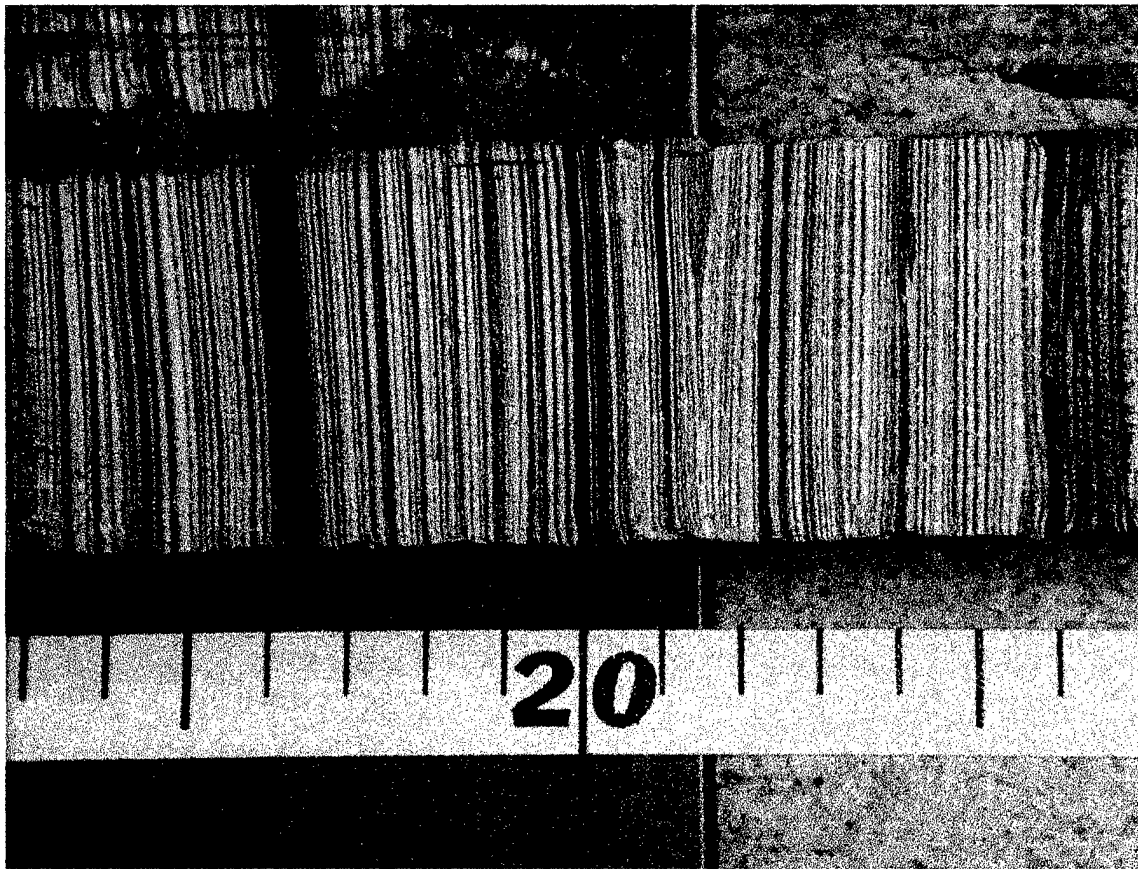
Fig 5. Close-up view of sediment layering in Lisan Core 3 Section 1115-1125cm.

calculated by graphing the AMS ages by depth, and then calculating a regression equation.

X-Ray Diffraction (XRD) Analysis

XRD analysis was used to identify major mineral phases before running oxygen and carbon isotope analyses. Eighteen aragonite samples were analyzed using XRD to determine carbonate mineral phase throughout the cores. Nine additional laminations did not contain enough material for both XRD analysis, and the subsequent isotopic analysis. Therefore, in these situations only isotopic analysis was performed. The core material was comprised of loose sediment. Thus, the dry sample material was crushed into a powder and then applied with an airbrush to a microscope slide using a Vaseline and hexane mixture. Halite residue was removed by rinsing with distilled water to increase result accuracy (Katz *et al.*, 1977). Halite was removed from samples to reduce the likelihood of reacting with the phosphoric acid and to ensure that no extraneous CO_2 was released from the halite which could alter the isotopic values extracted from the carbonate. XRD analysis was performed on a *Rigaku D/Max X-ray Diffractometer* operated by the Arizona State University Department of Chemistry. XRD settings were one scanning iteration and a scan speed of 2 and a scanning angle of 10-60°. Data interpretation was performed using a computer application provided by Rigaku for use with their D/Max X-ray

Generator. A hardcopy printout of each sample showing the phase peaks was created. However, the computer modeling software available at ASU did not contain the necessary code to determine quantitatively the mineral phases. Therefore, while XRD was used to analyze mineral phases present in the core, the precise percentages of those minerals were not determined.

Proton Induced X-Ray Emission (PIXE) Analysis

PIXE analysis was used to determine elemental sulfur content within laminae throughout Lisan Core 3. Sulfur was originally thought to be used as an indicator element to predict occurrence of evaporite mineralization, and thus, periods of greater hypersalinity than those periods in which carbonate minerals precipitated. Powdered or non-cohesive sediment was converted into eighteen sample pellets (Burnett et al., 1988). Material prepared for PIXE analysis was not used for XRD analysis due to crystallographic alteration of the minerals during pressing. The accelerator used for these analyses was a General Ionex 1.7MV Max. Terminal Voltage Tandetron (tandem design) Ion Accelerator operated by the Arizona State University Center for Solid State Science. The resulting computer output consisted of two products, a graphical representation of atomic composition, and a datasheet table showing elemental composition. Only the percent sulfur is used in this analysis.

Isotope Analyses

Oxygen and carbon isotope analysis is the key method for determining paleoclimates due to their ability to be used as proxies for past temperatures, and amounts of precipitation. Oxygen and carbon isotopes were analyzed from twenty-seven individual aragonite laminae using methods developed by McCrea (1950). Twenty-four samples were taken from Lisan Core 3; three samples were collected from near surface aragonite deposits in Dead Sea Core 3. The carbonate samples were first ground into a powder to insure a more complete reaction, then bleached in industrial grade Clorox bleach for 24 hours to remove organics that could have been washed/blown into the basin and deposited with the minerals, and finally rinsed with distilled water and filtered through a milipore filter. The remaining sample material was then reacted in a reaction vessel with H_3PO_4. Upon dissolving the sample material, CO_2 gas was separated from other gasses by cryogenic purification. Sulfate/sulfides were also removed by cryogenic purification, thus ensuring accurate isotopic results and decreasing the possibly of damage to the mass spectrometer. The remaining CO_2 gas was analyzed on a *3cm Nier Type Isotope Ratio Mass Spectrometer*, with the resulting interpretation being performed by Arizona State's Geological Science's Stable Isotope Lab. $\delta^{13}C$ data are presented relative to PDB standard. (PDB is a Creatceous belemnite, *Belemnitella americana*, from the Peedee formation of South Carolina (Craig, 1957), this source has since been exhausted and new

standards based upon this formation have been created using calcite). This standard is expressed as per mil (parts per thousand) and calculated as follows:

$$\delta(^{\circ}/_{oo}) = [\frac{R_{sample}}{R_{s\tan dard}} - 1] * 1000$$

$\delta^{18}O$ data were converted from PDB into the Standard Mean Ocean Water (SMOW) by the ASU's Stable Isotope Lab. To convert $\delta^{18}O$ from PDB into SMOW (for carbonates) can be done using the formula developed by Coplen et al., (1983):

$$\delta^{18}O_{SMOW} = 1.03091 * \delta^{18}O_{PDB} + 30.91$$

A paleotemperature calculation was determined from the $\delta^{18}O$ values using the formula from Craig, (1965):

$$t(c) = 16.9 - 4.2(\delta_c - \delta_w) + 0.13(\delta_c - \delta_w)^2$$

Where δ_c is the value of $\delta^{18}O$ within the CO_2 liberated by H_3PO_4, δ_w is the value of $\delta^{18}O$ within the CO_2 equilibrated at 25°C with water from which the carbonate has precipitated. A water value of 4.7 PDB (35.8 SMOW) (from Neev and Emery, 1967) were used as the δ_w value.

RESULTS

Age and Sedimentation Rates

Determining the age and rate of sedimentation within the Dead Sea was the key starting point of this study. Radiocarbon analysis by Beta Analytical Inc. was used to age date wood samples taken from Lisan Core 3 and Dead Sea Core 3. Sedimentation rates were then calculated using regression analysis.

AMS ages from wood in Lisan Core 3 (Table 1) and two wood samples from Dead Sea Core 3 (Table 2) produced age estimates with an accuracy of about +/- 70 yrs. Uncalibrated radiocarbon ages were used to calculate a sedimentation rate for Lisan Core 3 and Dead Sea Core 3. From the regression analysis a sedimentation rate of 13.8 yr/cm (0.73 mm/yr) was used to approximate sediment ages between 691-1,225 cm in Lisan Core 3 (Fig. 6). Thus, the sediments deposited between 691-1,225 cm represent the period from approximately 12.4-20.4kya uncalibrated radiocarbon yrs B.P. (years before present).

Because analyses of Dead Sea Core 3 deposits are only used to compare with results from Lisan Core 3 an age vs. depth graph is not produced for this core. (Using the surface of the Lisan Peninsula to approximate today, Dead Sea Core 3 would have a sedimentation rate of about 37.6 yr/cm or 0.27mm/yr).

Table 1. AMS ages from Lisan Core 3

Depth (cm)	Age (yrs B.P.)	Lab Number
698	12460+/-40	Beta – 153583
1,067	17990+/-60	Beta – 155308
1,186	19020+/-70	Beta – 156766

Table 2. AMS ages form Dead Sea Core 3

Depth (cm)	Age (yrs B.P.)	Calibrated Ages (yrs AD.)	Lab Number
45	1690+/-40	250-430	Beta – 153581
108	1820+/-40	100-206 and 290-320	Beta – 153582
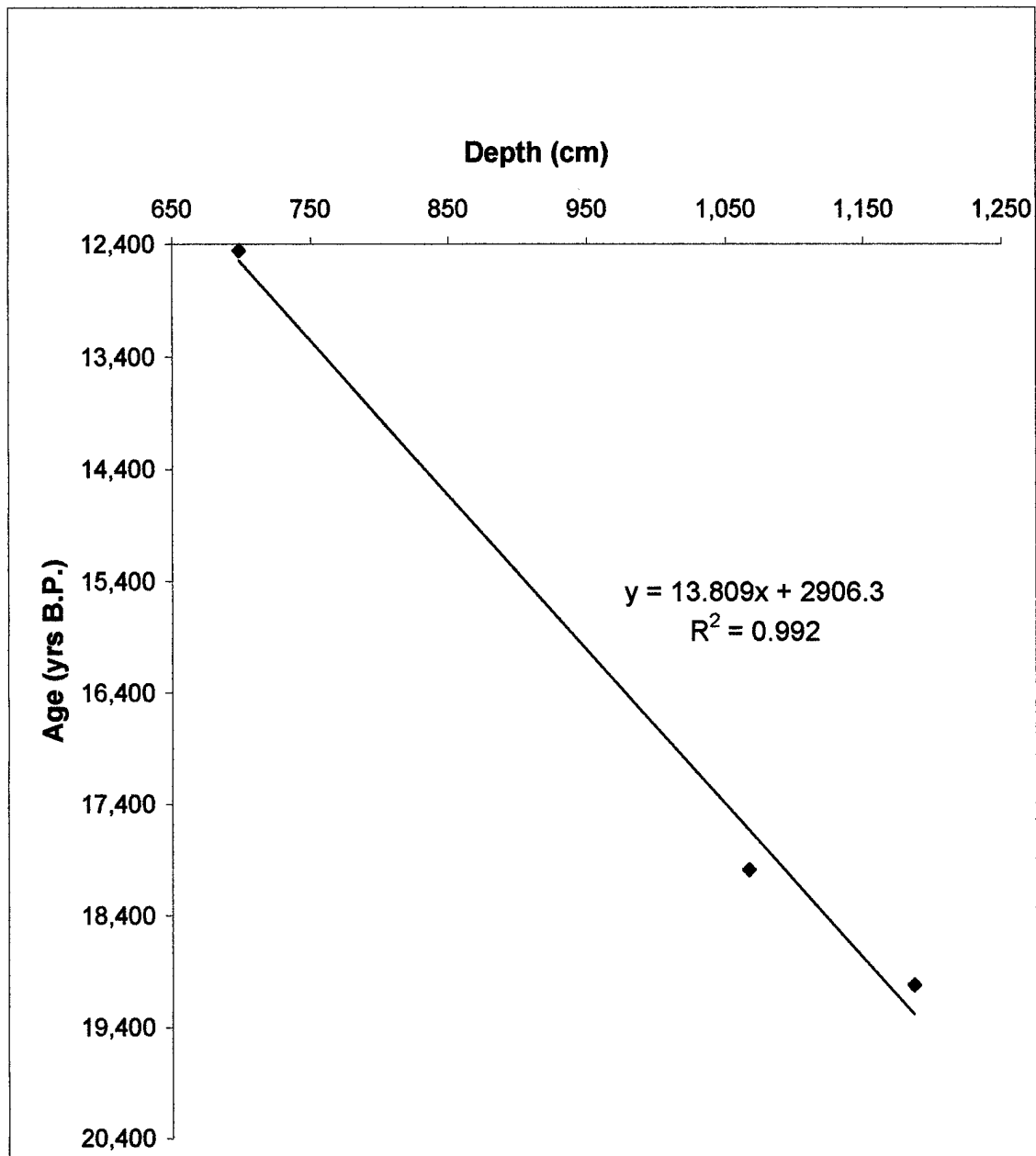
Fig 6. Age-depth relationship for Lisan Core 3.

X-Ray Diffraction (XRD) Analysis

XRD analyses of Lisan Core 3 were used to identify carbonate mineral phases in Lisan Core 3. XRD showed that all white layers analyzed were comprised mainly of aragonite, with trace amounts of gypsum, anhydrite, calcite and salts present as trace minor phases in portions of the core. Knowing what mineral phases were present provided a general picture of the hydrochemistry of the Dead Sea when those mineral phases formed. For example, precipitated aragonite indicates a different depositional environment than one in which halite or gypsum/anhydrite were precipitated. Table 3 shows the location of mineral phases. Aragonite was the dominant mineral phase throughout the Lisan Core 3, but evaporite minerals (gypsum and anhydrite) were present in two samples, at depths of 754cm and 826cm. Halite occurs at depths of 826cm, 855.5cm and 928.5cm.

Proton Induced X-Ray Emission (PIXE) Analysis

PIXE was used to determine atomic sulfur percentages in Lisan Core 3. Sulfur was originally used as an indicator element to predict occurrence of evaporite mineralization, and thus, periods of hypersalinity. Measured sulfur percentages are presented in Table 4. Percent of sulfur shows a peak at about 17.4kya with a maximum of 52% sulfur at 14.9kya (Fig. 7). Substantial amounts of sulfur occur in the core between 14.5-12.5kya (Table 4).

Table 3, Mineral phase location in Lisan Core 3

Core	Depth	Aragonite	Gypsum	Halite	Other
DS 3	Surface			X	
DS 3	37.5	X			
DS 3	46	X			
DS 3	53	X			Huntite
LS 3	691	X			Calcite, dolomite
LS 3	715.5	X			
LS 3	754.5	X	X		Calcite
LS 3	826	X	X	X	
LS 3	855.5	X		X	
LS 3	885	X			
LS 3	928.5	X		X	
LS 3	948	X			
LS 3	972.5	X			
LS 3	992	X			
LS 3	1013	X			
LS 3	1055	X			Possible anhydrite?
LS 3	1075	X			
LS 3	1115.5	X			
LS 3	1150	X			Calcite
LS 3	1189.5	X			
LS 3	1219	X			

Table 4. Percentage of sulfur by depth in Lisan Core 3

Age	Depth	% Sulfur
12,363	691	0.2%
12,515	702	14.0%
12,639	711	5.0%
13,032	739.5	15.0%
13,419	767.5	16.0%
13,867	800	16.0%
14,074	815	26.0%
14,088	816	13.0%
14,509	846.5	52.0%
14,916	876	0.3%
15,641	928.5	0.1%
16,130	964	0.2%
16,558	995	27.0%
17,041	1030	0.2%
17,386	1055	0.1%
17,828	1087	0.1%
19,042	1175	0.1%
19,242	1189.5	0.1%
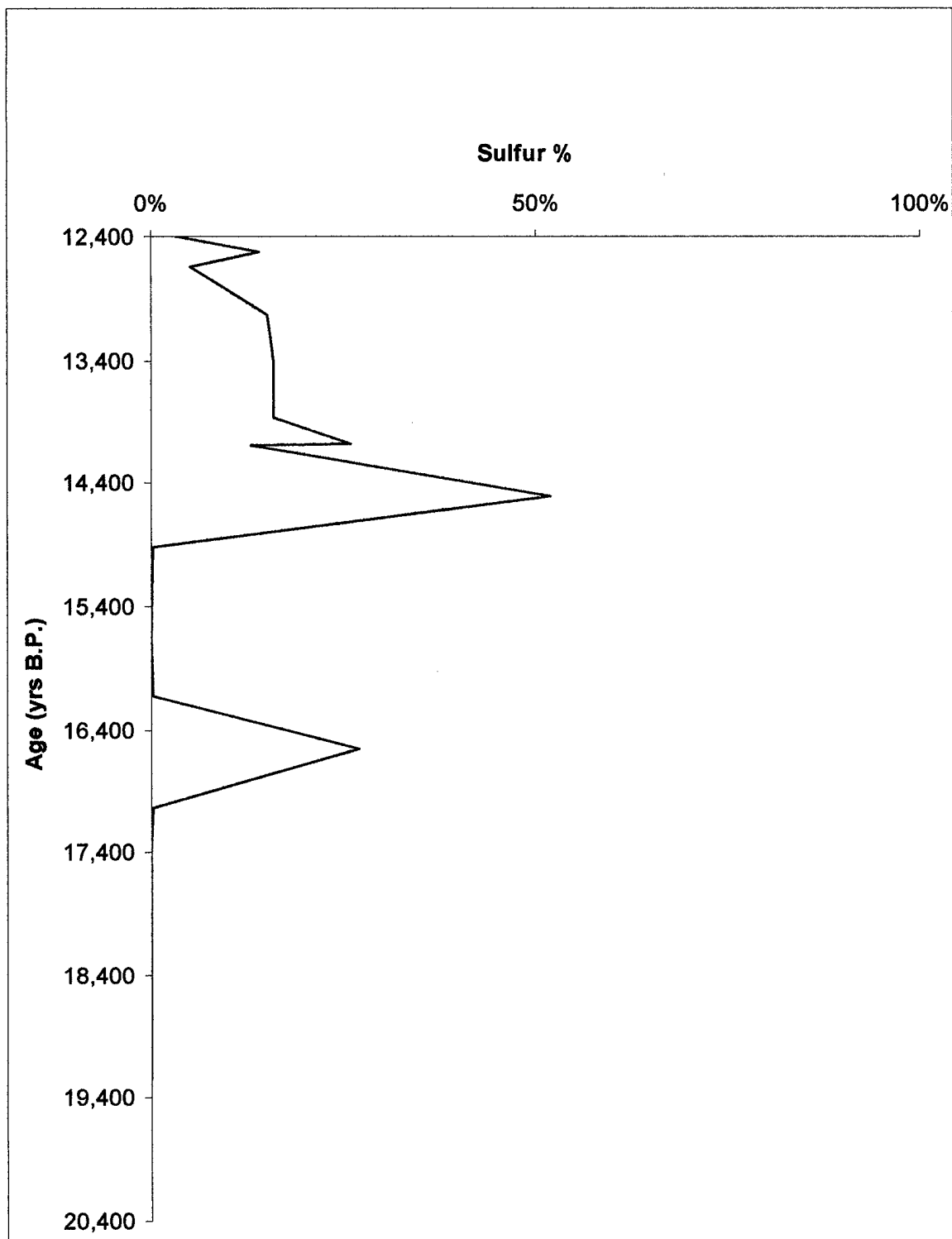
Fig 7. Percent sulfur in Lisan Core 3.

Sulfur spikes correspond to periods of dillution of both ^{13}C and ^{18}O. Regression analysis was performed on percentages of sulfur and $\delta^{13}C$ (Fig 8), $\delta^{18}O$ (Fig. 9).

Isotope Analyses

Carbon isotopes were used to show precipitation (as well as fluvial run-off) fluctuations due to their sensitivity to changes in ^{13}C enrichment. Hopes of accurate paleotemperature data was abandoned because without precise $\delta^{18}O$ values for the waters in which the carbonates precipitated, a definite temperature is not possible. Since the δ_w number used was derived from modern water, the isotopic composition was incorrect for periods of dilution, therefore, temperatures calculated with this δ_w values (4.7 PDB) rendered to warm a temperature during the period of dilution from 14.2-12.5 kya. Therefore, paleotemperature calculations are shown as relative and not absolute numbers (Fig 10).
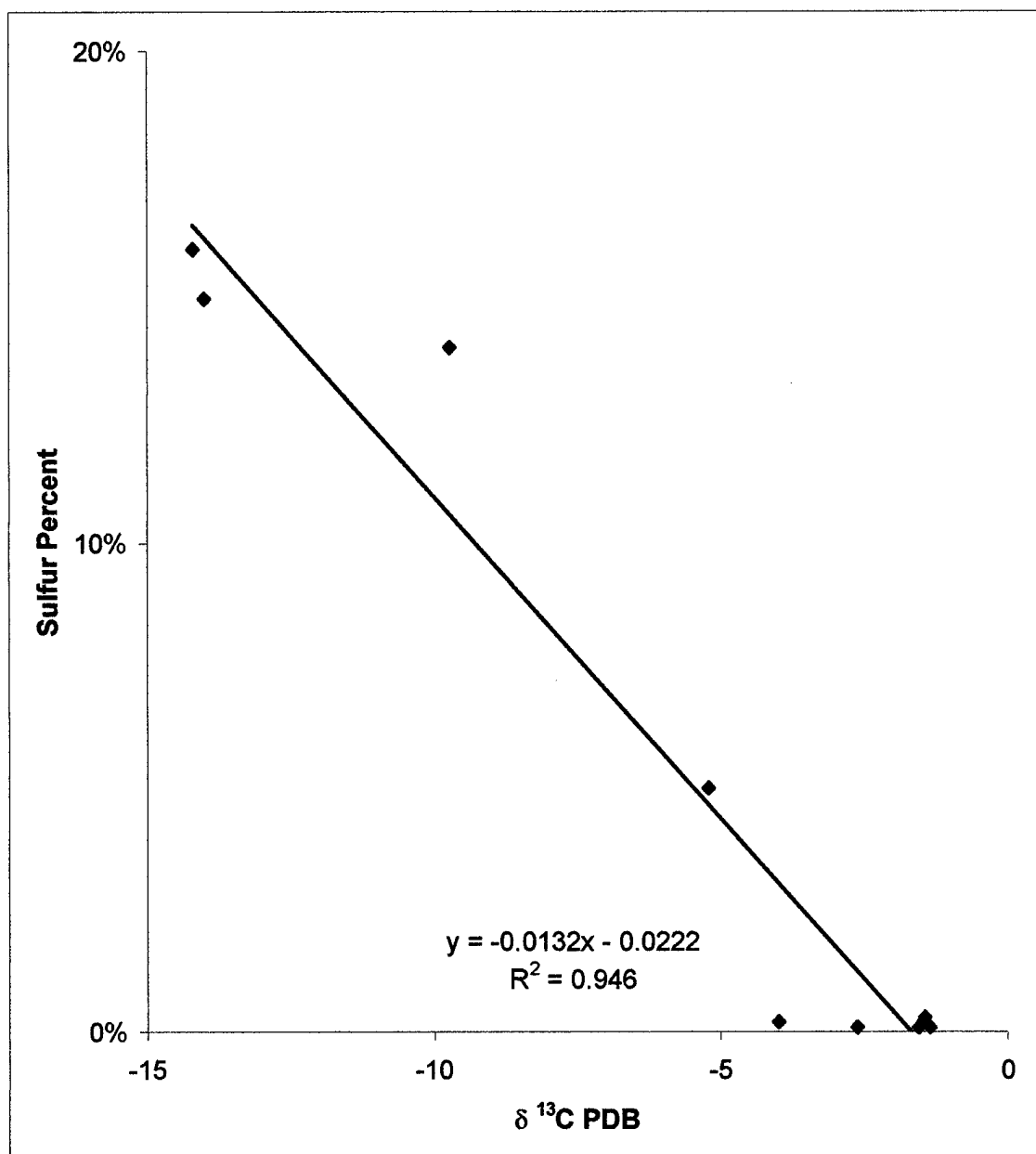
Fig 8. Regression analysis of $\delta^{13}C$ and sulfur.
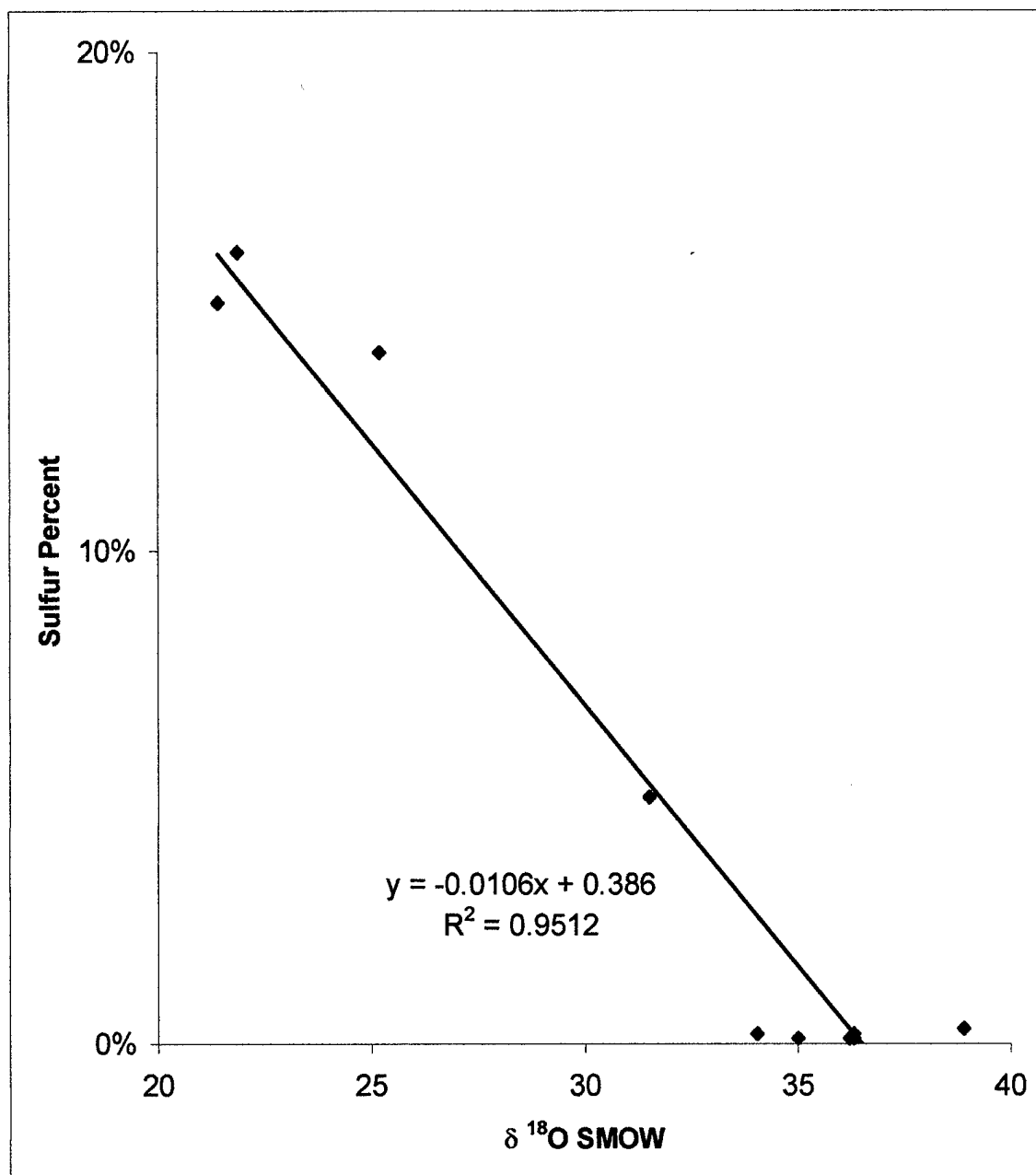
Fig 9. Regression analysis of $\delta^{18}O$ and sulfur.
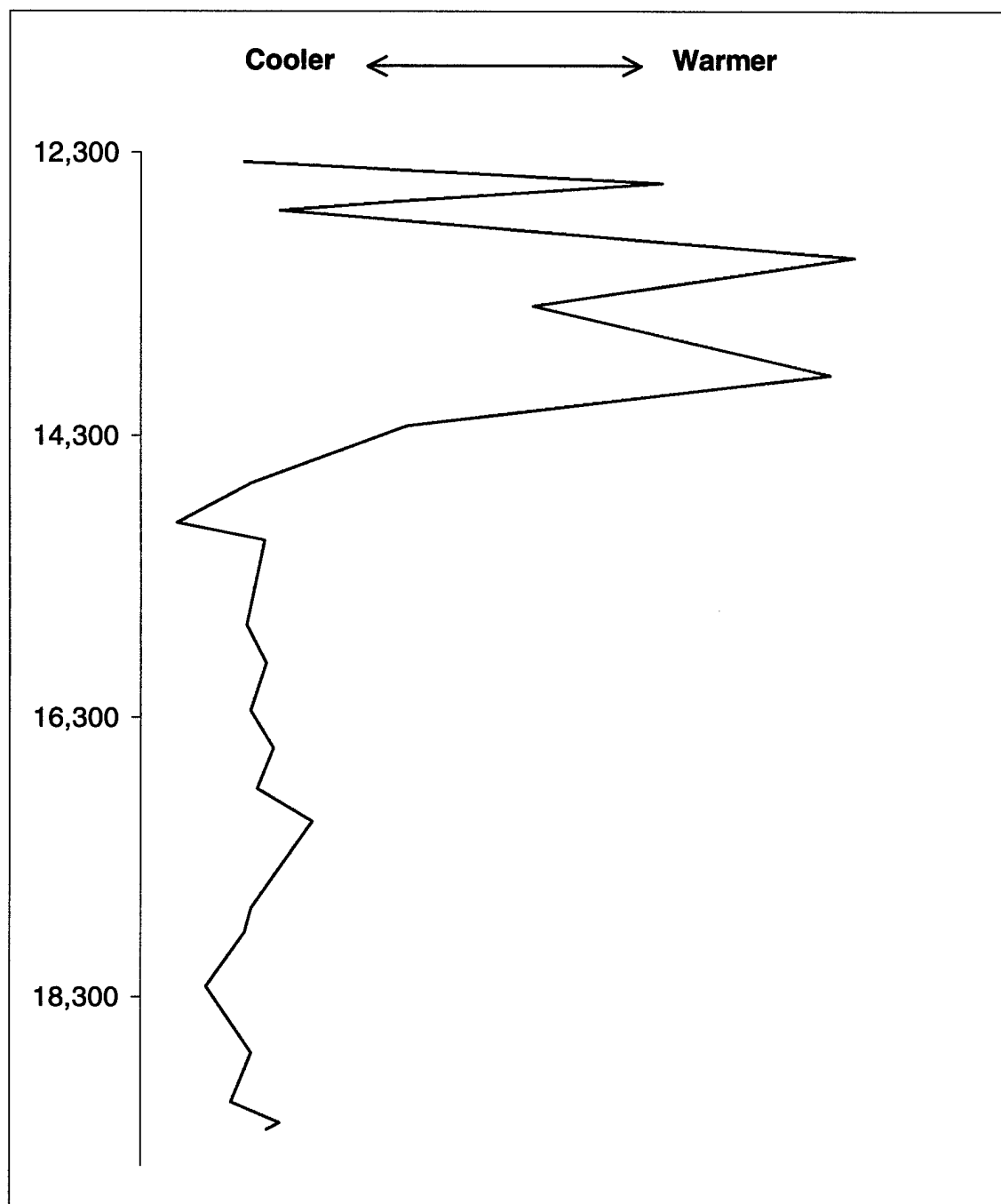
Fig 10. Age vs. relative temperature for Lisan Core 3.

Isotope analysis performed on aragonite minerals showed excellent correlation between $\delta^{13}C$ and $\delta^{18}O$ (Fig 11). Table 5 shows the results for Lisan Core 3; Table 6 shows results from Dead Sea Core 3. Values for $\delta^{18}O$ are shown as SMOW and range from 21 to 39. Whereas, values for $\delta^{13}C$ range from −14.2 to +1.6 PDB. Modern Jordan River water $\delta^{13}C$ values average −7.2 PDB (Stiller, 1974). Individual plots of $\delta^{13}C$ and $\delta^{18}O$ show a dramatic shift at roughly 14.5 kya (Figures 12 and 13). This strong shift by both ^{13}C and ^{18}O shows a diluting of both isotopes on a large scale. Dilution of this magnitude would require considerable organic debris to be washed into the basin, given the isotopic composition of the freshwater entering the basin from the Jordan River (-7.2 PDB, and −2.9 SMOW, Stiller et al., 1974; Katz et al., 1977).

Dead Sea Core 3 demonstrates values closer to today's composition. An average $\delta^{13}C$ value of −0.4 PDB and $\delta^{18}O$ value of 32.9 SMOW show values similar to today's Dead Sea isotopic composition. Barkan et al., (2000) recorded $\delta^{13}C$ values between 0.52-4.0 over the period of their study. Since the Dead Sea samples contain considerable halite, we can assume a lake level of −400 m msl or below. But since the average value for Dead Sea Core 3 is less enriched then the lowest ^{13}C value from Barkan et al., (2000), the Dead Sea must show great enrichment today than during the period encompassed by Dead Sea Core 3.
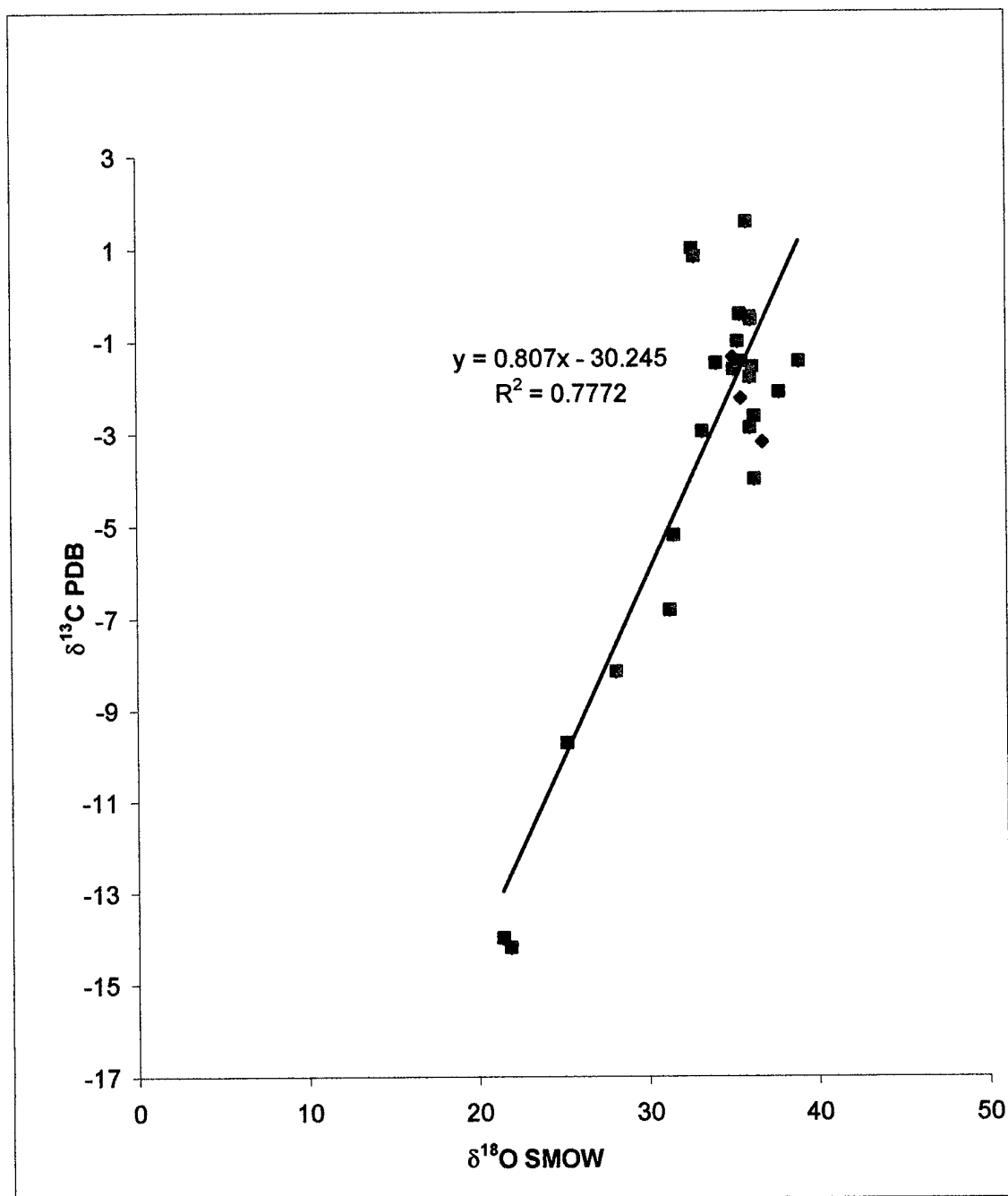
Fig 11. Regression analysis of $\delta^{18}O$ and $\delta^{13}C$.

Table 5. Carbon and oxygen isotope data for Lisan Core 3.

Depth (cm)	Age (yrs B.P.)	$d^{13}C$ (PDB)	$d^{18}O$ (SMOW)
691	12,363	-4.0	36.3
702	12,515	-9.7	25.2
711	12,639	-5.2	31.5
716	12,702	-1.6	35.1
740	13,033	-14.0	21.4
765	13,378	-8.2	28.1
800	13,868	-14.2	21.9
826	14,226	-6.8	31.3
856	14,634	-0.5	36.1
876	14,916	-1.5	38.9
885	15,041	-0.4	35.5
929	15,641	-1.6	36.2
948	15,910	-1.5	35.5
973	16,248	-0.5	36.1
992	16,517	-1.0	35.3
1,013	16,807	1.6	35.9
1,030	17,042	-1.5	34.0
1,075	17,663	-2.9	36.1
1,088	17,835	-2.6	36.3
1,116	18,222	-2.1	37.8
1,150	18,698	-1.8	36.1
1,176	19,050	-3.2	36.8
1,190	19,194	-1.4	35.0
1,219	19,243	-2.2	35.5

Table 6. Carbon and oxygen isotope data for Dead Sea Core 3.

Depth (cm)	Age (yrs B.P.)	d13C (PDB)	d18O (SMOW)
37.5	3,345	-3.0	33.2
46.0	3,462	1.0	32.6
53.0	3,559	0.8	32.8
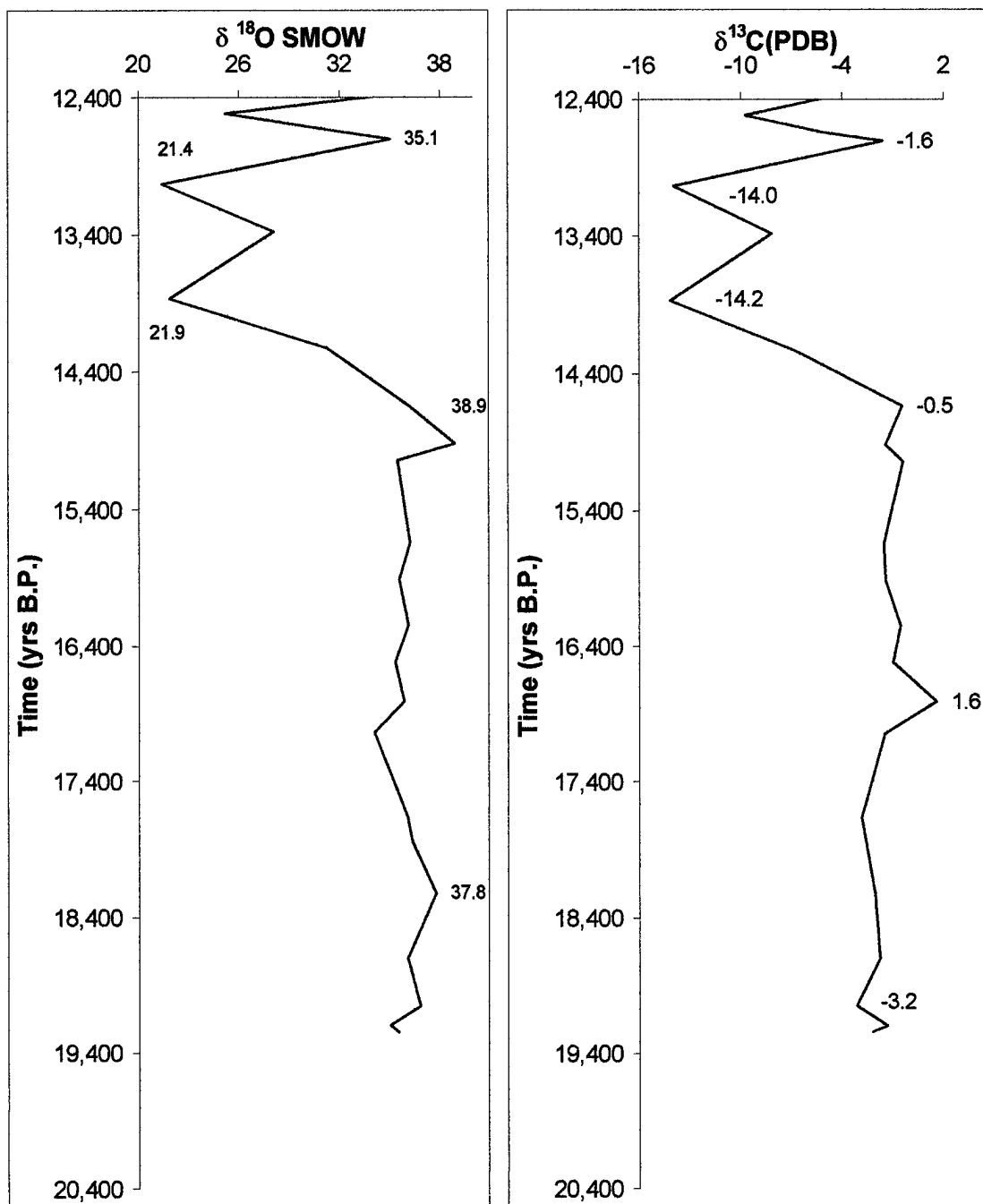
Fig 12 $\delta^{18}O$ (SMOW) changes through time for Lisan Core 3.

Fig 13. $\delta^{13}C$ (PDB) changes through time for Lisan Core 3.

DISCUSSION

This study focuses on interpreting the paleoclimate of the Dead Sea Basin by unlocking the carbon and oxygen isotope record, and by deciphering these data in the context of dynamic lake chemistry for which the Dead Sea is famous. The resulting story is then compared to other paleoclimate studies in this region that focused on palynology, geology, geomorphology and geochemistry.

Sedimentation Rate and Tectonic Activity

A sedimentation rate of 13.8 yr/cm (0.73mm/yr) was calculated using regression analysis based on AMS dates derived from wood samples taken from Lisan Core 3 and Dead Sea Core 3. This sedimentation rate is similar to rates derived from other studies. Schramm *et al.*, (1997) reported a sedimentation rate of 0.84mm/yr for the southwestern portion of the Dead Sea, and Gardosh *et al.*, (1990) calculated a rate of 0.83mm/yr. In addition, neither Lisan Core 3 nor Dead Sea Core 3 showed signs of tectonic activity. No slumping, overturn or disruption of the sedimentation was evident in either core. Thus, it is assumed that over the time periods when these cores were deposited (20-12 kya and around 1.6 kya) little or no tectonic activity occurred under the Lisan Peninsula. Research by Neev and Emery over a number of years (1967, 1995) has been interpreted as a draw off of Dead Sea waters due to tectonic subsidence of the

northern basin. This left the central lake basin as an elevated block (Abed and Yaghan, 2000). On-going tectonic subsidence as suggested by Neev and Emery (1967) cannot be refuted by observing the cores of this study. However, if subsidence were occurring only in the northern basin as Neev and Emery suggest, one would expect to see a possible mineralogical change in cores taken from the northern portion of the basin vs. cores taken from the Lisan Peninsula. As water was theoretically drawn into the northern basin, aragonite and calcite would continue to be deposited as calcium and bicarbonate mixed in the northern basin. However, the Lisan Peninsula would have been left as a shallower location as water slowly flowed into the deepening northern-most basin. As this process occurred, water temperatures would have increased over the shallower Lisan Peninsula, causing an increase in gypsum and anhydrite (evaporite) precipitation. Given these assumptions, and that precipitation held relatively stable, one would expect to see an increased percentage of evaporite minerals in Lisan Core 3, and a decreasing sedimentation rate. Nether of these two situations manifest themselves in Lisan Core 3, the sedimentation rate remains fairly constant over the length of the core, and elemental sulfur content does not proportionally increase, rather it peaks four times throughout the core. This evidence is not strong enough to refute Neev and Emery's claim, but does point in a direction for further research.

Carbon Isotopes

Carbon isotopes were chosen for study for their ability to demonstrate variability in precipitation/fluvial run-off coming into the Dead Sea Basin. For this report, enrichment is defined as Dead Sea water with $^{13}C/^{12}C$ ratios containing higher ^{13}C values than the modern Jordan River (-7.2 PDB) as provided by Stiller *et al.* (1974). Thus, values between -7.2 and 1.57 PDB are interpreted as enriched in ^{13}C. Dilution for this study is defined as Dead Seawater that contains less ^{13}C than the value reported by Stiller *et al.* (1974). Dilution values vary from -14.2 to -7.2 PDB.

Carbon Isotopes from Lisan Core 3 show considerable enrichment for the period between 20-14 kya, as would be expected for a hypersaline lake. From 19.5-16.9 kya ^{13}C values remained stable, averaging -2.2 PDB. A small enrichment event occurred at 16.9 kya that resulted in a ^{13}C value of +1.6 PDB. From 16.4-14.6 kya values averaged -1.0 PDB. Surprisingly, extreme enrichment as described by Stiller *et al.* (1985) was not evident in the Lisan Core 3 record. Stiller *et al.*, (1985) recorded values as enriched as +16.5 PDB in solar evaporation ponds within the modern southern basin. From this comparison it can be assumed that the waters over the Lisan Peninsula between 20-14 kya did not become shallow enough to produce these extreme enrichment values.

Four samples showed ^{13}C values more dilute than the modern Jordan River. These samples represent the time period from 13.8-13.0 kya and then at

12.5 kya. These dilution events are interpreted to represent the influx of organic material into the Dead Sea Basin through flood events. Organic carbonate formation and/or strictly freshwater influx would not dilute the ^{13}C PDB record enough to reach these numbers. Freshwater influx no matter how great would not dilute the Dead Sea waters greater than the normal δ^{13}C PDB readings for the Jordan River (-7.2 PDB). If a sudden influx of freshwater created an algae bloom, or increased the likelihood of organic carbonate production within the Dead Sea, normal values would still not reach those recorded in Lisan Core 3 sediments. Only an influx of washed in organic matter would dilute the ^{13}C PDB record sufficiently to explain these values.

Climate Interpretation Based on Carbon Isotopes

The paleoclimate from 19.5-12.4 kya is interpreted from δ^{13}C values from Lisan Core 3. Based upon these dilution events recorded in Lisan Core 3, it is hypothesized that the period 19.5-14.2 kya had a relatively stable climate. These relatively dry conditions from 19.5-14.2 kya, shifted to a wet environment from about 14.2-12.5 kya. Increased precipitation after 14 kya is suggested to have increased vegetation in the watershed. This expansion of vegetation probably resulted in increases organic material being washed into the Dead Sea Basin. This interpretation supports the research of Abed and Yaghan (2000), and refutes the work of Neev and Emery (1995). No evidence for a pluvial climate

during the period 20-14.2 kya, as suggested by Neev and Emery (1995), was seen in the $\delta^{13}C$ record. The younger Dead Sea Core 3 represents more near modern values (average ^{13}C values of -.4 PDB), demonstrating a return to a drier climate, more representative of today's Dead Sea environment. Further, paleoclimatic comparisons with other studies follow in subsequent sections.

Oxygen Isotopes

Oxygen isotopes were originally used to provide insight into the paleotemperature of the Dead Sea Basin, and to provide additional support for carbon isotopes. Comparison of oxygen and carbon isotopes proved to be successful, however the creation of a paleotemperature scale was successful only as relative temperatures, in terms of absolute temperatures was unsuccessful.

Katz *et al.* (1977) reported an average $\delta^{18}O$ value for the Jordan River to be –2.9 SMOW (-3.1 PDB). The change of standard conversion for water SMOW values differs from the conversion equation for lattice carbonates. The change of standard equation for water is:

$$\delta_{x-SMOW} = \delta_{x-PDB} + \frac{\delta_{x-PDB}\delta_{PDB-SMOW}}{10^3}$$

where x equals the δ ^{18}O value (in PDB) of the water sample. For lattice carbonates, values were converted from PDB units to SMOW units using the formula from Coplen *et al.* (1983):

$$\delta^{18}O_{SMOW} = 1.03091*^{18}O_{PDB} + 30.91$$

^{18}O values for Lisan Core 3 shows the same enrichment and dilution seen in the ^{13}C data.

Using the paleotemperature formula developed by Craig (1965) Temperatures as high as 100°C were calculated from the dilute ^{18}O values. Therefore, absolute paleotemperature calculations derived from precipitated aragonite in Lisan Core 3 would be highly inaccurate. This inaccuracy is a result of the unknown values of δ_w through time. The paleotemperature formula requires an isotopic value be calculated from the water in which the carbonate formed. Without an accurate δ_w value, a modern value must be substituted for paleotemperature calculations. For example, Neev and Emery (1967) used a sample δ_w value of 4.7 PDB (4.9 SMOW) (this value was originally given in PDB per Neev and Emery (1967) the SMOW conversion is present for convenience) derived from water sampled during their study. This value, although possibly relevant for the dry period from 20-14.6 kya, would be much less applicable for the dilute period between 14.2-12.5 kya. Undoubtedly much different water values would have been present during this wetter period. For example, if this

dilution period was caused by the melting of snow in the mountains to the north, the Jordan River water could have been diluted to ^{18}O values as low as –9.0 SMOW. This is highly unlikely the water would have stayed this dilute, give the distance the melt water would travel to the Dead Sea, increasing its ^{18}O values as the water continually evaporated. Certainly, values were lower during this period than the values obtained by Neev and Emery (1967). Temperatures calculated for the period 19.5-14.6 kya appear to be within modern documented temperatures. Temperature values for this period range from a low of 5°C to a high of 24°C. Values shown in Figure 10 demonstrate a relative temperature shift from a cooler, dry period (19.5-14.6 kya) to a warmer, wetter period (14.2-12.4 kya). This paleotemperature cure provides an estimate of the relative temperature estimate for the Dead Sea Basin.

Lake Chemistry

Carbon Dioxide Dynamics

The Dead Sea represents a unique natural laboratory due to its near lifelessness. This lack of a natural organic input allows a more precise ability to study the carbon cycle in nature. Understanding of this carbon cycle would allow for a better understanding of how and when carbonate minerals precipitate.

Barkan *et al.*, (2001) studied the physical and chemical paths of the carbon cycle in the Dead Sea during a flooding event that occurred during the winter of 1992. The authors presented two main points of interest, first, they suggest aragonite precipitation occurs during winter flood events when Ca^{2+} from within the Dead Sea and HCO_3^- brought in by flood waters mix, causing the precipitation of aragonite. Secondly, they state that since the present carbonate precipitation rate is approximately sixfold lower today than the average carbonate precipitation rate during the Lisan period (60-18 kya) (Kaufman, 1971), signifying a wetter period in the past. The authors stipulate that it is possible that evaporation was the driving factor in aragonite precipitation during the Lisan period. Whereas now, HCO_3^- influx during flood events drive carbonate precipitation. Based upon the isotopic record, and observations of the laminations in Lisan Core 3, it is possible aragonite precipitation occurred during winter flood events, but no evidence is visible for a wetter period during the Late Pleistocene as suggested by Barkan *et al.*, (2001). Therefore, given that aragonite was the dominant mineral phase during wet (winter) periods, one would infer a stratigraphic record of more dominate gypsum mineralization during the Late Pleistocene. However, Lisan Core 3 demonstrates clearly, that aragonite is the major mineral phase, even though precipitation has been shown in this study to be reduced to near modern levels. This would imply a different mechanism for precipitation of carbonate mineralization during the Late Pleistocene. Laboratory research by Bearat, (1992) demonstrated that with

limited CO_2 calcite would alter to aragonite in seawater. This possibility and the mechanism that drives this alteration require further study. Most likely, over the history of the Dead Sea, evaporation was the driving mechanism during the Late Pleistocene.

Gypsum, Sulfur, Halite and Aragonite Precipitation

The occurrence and location of carbonate and evaporite minerals can play an important role in determining the paleoenvironmental conditions present within the Dead Sea Basin. Neev and Emery (1995) indicate that the Dead Sea precipitates mainly halite when its surface reaches –400m msl or lower. Halite precipitation has been used as a mineralogical indicator of paleolake levels through this theory. Halite was present in three samples of Lisan Core 3 that were analyzed using XRD: 826 cm, 855.5 cm and 928.5 cm. The presence of halite occurred over the period 15.6-14.2 kya, whereas, isotopic enrichment occurred at 16.8 kya. Evaporite mineralization (gypsum and anhydrite) occurred at three locations, two during the period from 14-13 kya, squarely in the middle of the greatest extent of isotopic dilution. Elemental sulfur percentage as determined by PIXE analysis (see table 4) showed sulfur spikes at 16.6 kya (26%), 14.5 kya (52%) and 14.1 kya (27%). These spikes do not exactly match the maximum dilution of 16.8 kya, however increased sulfur content appears to equate to wetter conditions, which then could represent increased biotic life

within the Dead Sea. Bacteria blooming during periods of increased freshwater could reduce sulfates in the water into elemental sulfur blems. Such blems were found throughout Lisan Core 3.

Unfortunately, all samples were not able to be analyzed using XRD due to the amount of sample present in laminations. Samples without enough material for XRD and isotopic analysis were analyzed for isotopic ratios only.

Paleolake Levels

Paleolake levels for the Dead Sea Basin have varied from a high stand of −180m (Neev and Emery, 1967; Begin *et al.*, 1974) to its current surface of −404m msl (mean sea level). Horowitz (1992) describes the greatest extent of the Dead Sea to have occurred during the period from 32-22 kya. By 22-18 kya, the lake had shrunk to −240m msl (Niemi, 1997; Horowitz, 1992). A return to wetter conditions occurred around 17-15 kya when the Dead Sea reached its high stand of −180m msl (Niemi, 1997). After this high stand, the lake is hypothesized to have fallen to −700 m msl during the Holocene and the Dead Sea was likely a series of intermittent lakes (Niemi, 1997; Begin *et al.* 1985). Neev and Emery (1995) surmise that halite precipitated only when the lake level reached a critical level of −400 m msl. This corresponds to today's observations with halite the major mineral phase deposited at the current lake level of −404 m msl. Neev and Emery (1995) also created a gamma ray log that they correlated

to estimated radiocarbon ages extrapolated from other locations along the rift. Their work showed halite as the major mineral phase at approximately 15 kya, the period that Lisan Core 3 demonstrates some of the wettest conditions. Neev and Emery (1995) discuss the possible error induced in radiocarbon ages between carbonate and organic material within the Dead Sea.

Paleoclimate Correlations to Lisan Core 3

Numerous studies have been undertaken to understand the paleoclimate of Southern Levant using a variety of methods, such as palynology, geology, archeology, geochemistry, and even astronomy (Table 7). Different views on whether the paleoclimate of the Southern Levant was wet or dry during the late Pleistocene exist with no clear agreement on the climate of the LGM. These discrepancies could result from varying climates within the specific region of each study. For example, climatic conditions were variable during the LGM, and paleoprecipitation patterns need not match worldwide. However, discussion will focus on climatic interpretations of the Levant and a lesser part, Africa.

Isotopic analysis from this study supports the idea of a dry LGM, with fluvial conditions peaking at 13.8 kya. Neev and Emery (1995) depict through gamma log analysis, the period 20-17 kya to be pluvial, but dry from 17-15 kya. However, Dead Sea Basin levels fluctuated dramatically during this period. One

high stand of the Dead Sea occurs at 14.6 kya (Druckman, Marrgaritz and Sneh, 1987).

Abed and Yaghan (2000) discuss the paleoclimate of the Dead Sea Basin, from a stratagraphic perspective. This study's results support their findings, that of a dry LGM from 20-15 kya, with a wet period from 15-11 kya (Abed and Yaghan, 2000).

Table 7, Paleoclimate comparison

Researcher	20-15 kya	15-11 kya	Locale	Basis for Interpretation
Swoveland (2001)	Dry	Wettest at 13.8 kya	Dead Sea	δ^{13}C and δ^{18}O Isotopes
Neev and Emery (1995)	Wet 20-17 kya Dry 17-15 kya	?	Dead Sea	Gamma Ray Log
Abed and Yaghan (2000)	Dry	Wet	Dead Sea	Sedimentology
Perry and Hsu (2000)	Dry (full glacial)	Wet (interglacial at 14 kya)	Global	Solar output model
Yan and Petit-Maire (1994)	Dry	Dry (wet occurs 8.5-7 kya)	Southern Sahara-Sahel	Geologoical, paleobiological and archaeological
Hooghiemstra (1987)	Dry	Fluvial spike at 13 kya	NW Africa	Marine pollen
Van Campo (1986)	Dry	Very humid culminates at 11 kya	SW India	Oxygen isotope and pollen
Baruch and Bottema (1991)	Dry	Humid culminates at 13 kya	Hula Basin, Israel	Palynological
Grazzini (1975)	Dry	Most dilute δ^{18}O values at about 13 kya	Mediterranean Sea	Oxygen isotope in Foraminifera
Roberts and Wright (1993)	Dry	Pollen peak at 9 kya	Ghab depression	Pollen
Horowitz (1979)	Humid (both cool and warm)	Humid through 11.5 kya	Hula Valley	Pollen

Perry and Hsu (2000) correlated solar-output to geophysical, archaeological and historical evidence. Their interpretation of the global paleoclimate supports a warming period about 15 kya (Perry and Hsu, 2000). Unfortunately, their research does not focus on the Southern Levant, therefore their predictions do not account for the variability monsoonal or Mediterranean rains could have forced on the climate of the Dead Sea from the LGM through the Holocene.

Yan and Petit-Maire (1994) reviewed the continental changes along the African and Asian monsoon transitional zones during the last 140 kyr. Their findings support two wet episodes at 55 and 22 kya (Yan and Petit-Maire, 1994). A severe arid phase was associated with the LGM generally between 21-15 kya is suggested (Yan and Petit-Maire, 1994). According to the authors, monsoonal margins experienced a minor temperature decrease and a major rainfall decrease over this period (21-15 kya).

Similarly, Hooghiemstra (1988) described the major wind belts and resulting vegetation zones in NW Africa from 20-5 kya, as interpreted from marine pollen records. During the period 19-14 kya a compressed savanna belt extended between about 12° and 14-15°N. The Sahara desert reached its maximum extent due to hyperarid conditions (Hooghiemstra, 1988). By about 13 kya, the trade winds weakened, and after 14 kya the climate became less arid south of the Sahara and a first fluvial run-off spike occurred around 13 kya.

Fluvial run-off continued to increase from 11 kya on, reaching its maximum at 9-7.8 kya. This relates well the isotopic results from this study.

Van Campo (1985) studied oxygen isotope and pollen evidence off Southwest India, and derived similar climatic conditions as Hooghiemstra and as this study. Van Campo (1985) described two phases of the climate of Southwest India as an arid period from 22-18 kya, followed by a very humid period culminating at 11 kya. The extension of the monsoon over India after the LGM was a gradual process following the northward progression of the Intertropical Convergence Zone (Van Campo, 1985). The author describes this very humid period to correspond to the highest pollen count, and it represents the maximum summer insolaton of the Northern Hemisphere.

Grazzini (1975) interpreted the $\delta^{18}O$ record found in Foraminifera carbonates in the Mediterranean Sea. While focused mainly on the temperature fluctuation over this time, the author also discusses dilution and enrichment of $\delta^{18}O$ based upon changing precipitation driven by climate change. $\delta^{18}O$ curves produced show a dilution maximum around 13 kya, with a relative enriched period from 20-13 kya.

Roberts and Wright (1993) offer a different interpretation from other pollen and vegetation studies in that their fluvial peak occurs later, at approximately 9 kya, well into the Holocene. In fact, the authors suggest the period from 15-13 kya was the most intensely arid period than any other during the last 30 kyr within southwest Asia (Roberts and Wright, 1993). The authors studied the Ghab

depression to determine the climatology of the Levant. Their core, a 7 m section that covered the past 50 kyr only contained one radiocarbon date. Thus, they inferred that by 9 kya the area was already well forested, but were unable to determine the exact timing for this period of increased precipitation and forest growth.

The Hula marsh showed steppe vegetation between 25-14 kya then an expansion of oak between 14-10 kya (Roberts and Wright, 1993). Similarly, Horowitz (1979) drew his interpretation from a pollen core from the Hula Valley. His interpretation showed cool, humid conditions existed from 18-16 kya with the landscape dominated by oak and olive forests. By 11.5 kya, the climate has begun to warm and dry with the majority of olive growth retreating (Horowitz, 1979). Baruch and Bottema (1991) used palynological evidence from the Ghab in northwestern Syria, and the Hula in northern Israel to describe the changing climate of the Levant from 17-9 kya. The authors describe a cool, dry period from 17-13 kya where land cover was mainly steppe and desert plants. At approximately 15 kya more humid conditions occurred, resulting in an gradual expansion of forest areas (Baruch and Bottema, 1991).

There appears to be general agreement that a dry climate in the Southern Levant existed from the LGM through approximately 15 kya. A short wetter period occurred around 14 kya with fluctuations until the much drier Holocene. These other studies on the paleoclimate of the Southern Levant support the research done through analysis of Lisan Core 3.

Climate fluctuations within the North African, Levant and India region correspond to global climate fluctuations that occurred during the last 140 kya (Yan and Petit-Maire, 1994). Global warm/cold cycles match global humid/arid cycles, with these cycles matching orbitally induced solar insolation forcings (Berger, *et al.*, 1992). The African, Indian and Asian monsoons were affected by these global climate fluctuations. Why significant revivals of the Asian monsoon occurred between the 15-10 kya are not clearly understood (Yan and Petit-Maire, 1994).

CONCLUSIONS

This study's main goal was to interpret the paleoclimate of the Dead Sea Basin from 20-12.4 kya. A relative paleotemperature curve shows a cool, dry period from 20-14.6 kya, and a warmer, wetter period from 14.2-12.5 kya. Paleoprecipitation determined from $\delta^{13}C$ values derived from carbonate (aragonite) were successful in producing an isotopic curve that indicated periods of increased freshwater influx. This curve was substantiated by research into the paleoclimate of the Southern Levant using palynology, geology, archeology and geochemistry. Although a few researchers conclude the period from 19.5-14.2 kya was wet and cold (Neev and Emery, 1967 1995), most studies concluded that this period was in fact relatively stable, cool and dry, with $\delta^{13}C$ values only slightly more dilute then modern readings in the Dead Sea. Values for this study show a constant climate from 19.5 kya through 14.6 kya. At about 14.6 kya the climate changed to one with increased amounts of precipitation which caused increased vegetation. It is hypothesized that organic matter was washed into the Dead Sea which can correlated to the dilution of carbon 13 recorded within Lisan Core 3. Dead Sea Core 3 values (-0.04 PDB) are similar to modern winter values, and show a return to a stable drier climate more representative of today's Dead Sea environment. In conclusion, this research suggests a climate dominated by dry conditions from 19.5-14.2 kya, with a shift to a wetter environment for the period from 14.2-12.5 kya.

REFERENCES

Abed, A.M., and Yaghan, R., 2000. On the paleoclimate of Jordan during the last glacial maximum. Palaeogeography, Palaeoclimatology, Palaeoecology, 160, 23-33.

Abu-Ajamieh, M.M., Bender, F.K., Eicher, R.N., El Kaysi, K.K., Nimri, F., Qudah, B. H., Qudah, B. H., and Sheyyab, K. H., 1989. Natural Resources in Jordan-Inventory, evaluation, development programs: Amman, Jordan. Natural Resources Authority, 1-224.

Abu-Jaber, N.S., Al-Bataina, B.A., and Ali, A.J., 1997. Radiochemistry of sediments from the southern Dead Sea, Jordan. Environmental Geology, 32, 281-284.

Anati, D. A., and Stiller, M., 1991. The post-1979 thermohaline structure of the Dead Sea and the role of double-diffusion mixing. Limnology and Oceanography, 36, 342-354.

Arieh, E, 1967. Seismicity of Israel and adjacent areas. Geologic Survey of Israel, Bull. 43, 1-14.

Barkan, Eugeni, Luz, Boaz, Lazar, Boaz, 2001. Dynamics of the carbon dioxide system in the Dead Sea, Geochimica et Cosmochimca Acta 65, 3, 355-368.

Begin, Z.B., Broecker, W., Buchbinder, B., Druckman, Y., Kaufman, A., Magaritz, M., and Neev, D., 1985. Dead Sea and Lake Lisan Levels in the last 30,000 years, a preliminary report: Jerusalem, Geological Survey of Israel, report 29/85, 1-18.

Berger, A., Loutre, M.F. Laskar, J., 1992. Stability of the astronomical frequencies over the Earth's history for paleoclimate studies. Science, 255, 560-566.

Béarat H., 1990. Etude de quelques altérations physico-chimiques des céramiques archéologiques, Ph.D. Dissertation, Caen University, France, published in microfiche No. CAEN/90/2011, Grenoble, France. Page:126.

Blackwelder, E., 1954. Geomorphic processes in the desert, California Division of Mines and Geology Bulletin 170, 11-20.

Bowman, D., 1993. Geomorphology of the Dead Sea Western Margin, The Dead Sea, The Lake and It's Settings. Oxford Monographs on Geology and Geophysics, 36, 1-286.

Broeker, W.S, and Denton, G.H., 1989. The role of ocean-atmosphere reorganization in glacial cycles. Geochimica et Cosmochimca Acta, 53, 2465-2501.

Burnett, D.S., Woolum, D.S., Benjamin, T.M., Rogers, P.S.Z., Duffy, C.J., and Maggiore, C., 1988. High precision thick target PIXE analysis of carbonaceous meteorites. Nuclear Instruments & Methods in Physics Research. B35, 67-74.

Cabri, L.J., 1988. Applications of proton and nuclear microprobes in ore deposit mineralogy and metallurgy, Nuclear Instruments & Methods in Physics Research, B30, 459-465.

Coplen, T.B., Dendall, C. and Hopple, J., 1983. Comparison of isotope reference samples. Nature, 302, 236.

Craig, H., 1957. Isotopic standards for carbon and oxygen and correction factors for mass-spectrometric analysis of carbon dioxide. Geochimica et Cosmochimca Acta. 12, 133-149.

Craig, H., 1965. The Measurement of Oxygen Isotope Paleotemperatures, Stable Isotopes in Oceanographic Studies and Paleotemperatures, Spoleto, July 26th-30th .

Currey, D.R., 1994. Hemiarid lake basins: Geomorphic Patterns, Geomorphology of Desert Environments, Chapman & Hall.

Davis, W.M., 1909. Geographical Cycle in an Arid Climate, Geographical Essays, 296-322.

Druckman, Y., Margaritz, M., and Sneh, A., 1987. The shrinking of Lisan Lake, as reflected by the digenesis of its marginal oolite deposits. Israel Journal of Earth Science, 36, 101-106.

Edwards, P.C., Falconer, S.E., Fall, P.L., Berelov, I., Meadows, J., Meegan, C., Metzger, M.C., and Sayej, G.J., in press, Archaeology and Environment of the Dead Sea Plain: preliminary results of the first season of investigation by the joint La Trobe University/Arizona State University Project., Annual of the Department of Antiquities of Jordan.

El-Naser, H. and Subah, A., 2000. Using hydrochemistry and environmental isotopes to define the groundwater system of the Ain Magnara Spring, Jordan, Engineering Geology and Hydrogeology, 33, 87-96.

Eyal, M., and Eyal, Y., and Heimann, A., 1990. The evolution of the Barahta rhomb-shaped graben, Mount Hermon, Dead Sea Rift, Tectonophysics, 180, 101-110.

Galassi, S., Provini, A., and Garofalo, E., 1992. Sediment analysis for the assessment of risk form organic pollutants in lakes, Hydrobiologia, 235/236 639-647.

Galusha, T., Johnson, N.M., Lindsay, E.H., Opdyke, N.D., and Tedford, R.H., 1984. Biostratigraphy and magnetostratigraphy, late Pliocene rock, 111 Ranch, Arizona, Geological Society of America Bulletin, 95, 714-722.

Garfunkel, Z., 1981. Internal structure of the Dead Sea leaky transform (rift) in relation to plate kinematics, Tectonphysics, 80, 81-108

Garfunkel, Z, 1993. Structure and Tectonics of the Dead Sea Basin, The Dead Sea, The Lake and It's Settings, Oxford Monographs on Geology and Geophysics, 36, 286.

Gilbert, G.K., 1880. Geology of the Henry Mountains, Washington, D.C. Government Printing Office.

Ginzburg, A., and Folkman, Y., 1980. The crustal structure between the Dead Sea rift and the Mediterranean Sea: Earth Planetary Science Letters, 51, 181-188.

Gregory, K.J., 2000. The changing Nature of Physical Geography, Arnold Publishing, 1-368.

Hare, F.K. 1983. Climate on the Desert Fringe, Mega-Geomorphology, R. Gardner and H. Scoging. Oxford, Clarendon Press, 134-151.

Hickmott, D., and Baldridge, W.S., 1995. Application of PIXE microanalysis to macerals and sulfides from the Lower Kittanning Coal of Western Pennsylvania. Economic Geology, 90, 246-254.

Horita, J., Gat, and Joel R., 1989. Deuterium in the Dead Sea: Remeasurement and implications for the isotopic activity correction in brines. Geochimica et Cosmochimca Acta, 53, 131-133.

Horowitz, A., 1979. The Quaternary of Israel, Academic Press, Inc., 1- 94.

Ingles, M., and Anadon, P., 1991. Relationship of clay minerals to depositional environment in the non-marine Eocene Pontils Group, Se Ebro Basin (Spain). Journal of Sedimentary Petrology, 61, 926-939.

Katz, A., Kolodny, Y., and Nissenbaum, A., 1977. The geochemical evolution of the Pleistocene Lake Lisan-Dead Sea system, Geochimica et Cosmochimica Acta, 41, 1609-1626.

Kaufman, A. 1971. U-series dating of Dead Sea basin carbonates. Geochimica et Cosmochimca Acta, 35, 1269-1281.

Kudrass, H.R., Erlenkeuser, H., Vollbrecht, R., and Weiss, W., 1991. Global nature of the Younger Dryas cooling event inferred from oxygen isotope data from Sulu Sea cores. Nature, 349, 406-409.

Klein, C., 1986. Fluctuations of the level of the Dead Sea and climatic fluctuations in Erez-Israel during historic times (in Hebrew), Ph.D dissertation, Jerusalem, Hebrew University Department of Geography.

Levy, Y., 1985. Modern halite precipitation in the Dead Sea, Geological Survey of Israel, Report No. GSI/7/85.

Machette, M.N., 1985. Calcic soils of the southwestern United States, Geological Society of America, Special Paper 203, 1-21.

McCrea, J.M., 1950. On the Isotopic Chemistry of Carbonates and a Paleotemperature Scale, The Journal of Chemical Physics, 18, 6, 849-857.

Munson, B., 1977. Chemical Ionization Mass Spectrometry, Analytical Chemistry, 49.

Neev, D., and Emery, K.O., 1967. The Dead Sea – Depositional Processes and Environments of Evaporites. Geologic Survey of Israel Bulletin, 41, 147.

Neev, D., and Emery, K.O., 1995. The Destruction of Sodom, Gomorrah, and Jericho. Oxford University Press, 175.

Niemi, T., 1997. Fluctuations of Late Pleistocene Lake Lisan in the Dead Sea Rift. The Dead Sea, The Lake and It's Settings. Oxford Monographs on Geology and Geophysics 36, 286.

Nishri, A., and Nissenbaum, A., 1993. Formation of manganese oxyhydroxides on Dead Sea coast by alteration of Mn-enriched carbonates, Hydrobiologia, 267, 61-73.

Nissenbaum, A, Stiller, M., and Nishri, A., 1990. Nutrient in pore waters from the Dead Sea sediments, Hydrobiologia, 197, 83-89.

Noller, J., 2000. Quaternary Geochronology, Methods and Application. AGU Reference Shelf. 4, 1-9.

Peglar, W., Fritz, S.C., Alapieti, T., Saarnisto, M., and Birks, J.B., 1984. Composition and formation of laminated sediments in Diss Mere, Norfork, England, Boreas, 13, 13-28.

Quevauviller, PH., Ure, A., Muntau, H., and Griepink, B., 1993. Improvement of analytical measurements within the BCR-Programme: single and sequential extraction procedures applied to soil and sediment analysis, Environmental Analytical Chemistry, 51, 129-134.

Rao, J.L., and Berner, R.A., 1995. Development of an electron microprobe method for the determination of phosphorus and associated elements in sediments, Chemical Geology, 125, 169-183.

Raymo, M.E., and Ruddiman, W.F., 1992. Tectonic forcing of late Cenozoic climate, Nature, 359, 117-122.

Ryan, C.G., and Griffin, W.L., 1993. The nuclear microprobe as a tool in geology and mineral exploration, Nuclear Instruments & Methods in Physics Research, B77, 381-398.

Schramm, A., Stein, M., and Goldstein, S.L., 2000. Calibration of the ^{14}C time scale >40 ka by $^{234}U - {}^{230}Th$ dating of Lake Lisan sediments (last glacial Dead Sea), Earth and Planetary Science Letters, 175, 27-40.

Shapira, A., On the Seismicity of the Dead Sea Basin, 1993, The Dead Sea, The Lake and It's Settings. Oxford Monographs on Geology and Geophysics. 36, 286.

Stein, M., Starinsky, A., Katz, A., Goldstein, S.L., Machlus, M., and Schramm, A., 1997. Strontium isotopic, chemical, and sedimentological evidence for the evolution of Lake Lisan and the Dead Sea, Geochimica et Cosmochimica Acta, 61, 3975-3992.

Stiller, M., Rounick, J. S., and Shasha, S., 1985. Extreme carbon-isotope enrichments in evaporating brines, Nature, 31,6 434-435.

Steinhorn, I., 1979. The Dead Sea: deepening of the mixolimnion signifies the overture to overturn of the water column, Science, 206, 55-57.

Steinhorn, I., and Assaf, G., 1980. The physical structure of the dead Sea water column, 1975-1977, In a. Nissenbaum (ed), Hypersaline Brines and Evaporitic Environments. Amsterdam, Elsevier, 145-153.

Stiller, M., and Chung, Y., 1984. RA-226 in the Dead Sea a possible tracer for the duration of meroximia, Limnol. Oceanogr. 29, 574-586.

Stiller, M., Nissenbaum, A., 1999. Geochemical investigation of phosphorus and nitrogen in the hypersaline Dead Sea. Geochimica et Cosmochimica Acta, 63, 3467-3475.

Swennen, R. and Van der Sluys, J., 1998. Zn, Pb, Cu and As distribution patters in overbank and medium-order stream sediment samples: their use in exploration and environmental geochemistry. Geochemical Exploration, 65, 27-45.

Willard, H.H., Merritt Jr., L,L., Dean, J.A., and Settle Jr., F.A., Instrumental Methods of Analysis, 1988. Wadsworth, Inc.

Wright, H.E. Jr., Kutzbach, J.E., Webb III, T., and Ruddiman, W.F., 1993. Global Climates since the Last Glacial Maximum, University of Minnesota Press.

Yechieli, Y., and Ronen, D., 1997. Early diagenesis of highly saline lake sediments after exposure, Chemical Geology, 138, 93-106.

Zilberman, E., Amit, R., Heimann, A., and Porat, N., 2000. Changes in Holocene Paloesiesmic activity in the Hula pull-apart basin, Dead Sea Rift, northern Israel, Tectonophysics, 321, 237-252.

ABSTRACT

The purpose of this study was to determine the late glacial paleoclimate of the Southern Levant. A study of $\delta^{13}C$ and $\delta^{18}O$ in carbonates (aragonite) was undertaken from a Lisan Core 3, a laminated core, collected from the Lisan Peninsula in the Dead Sea. Accelerator Mass Spectrometer (AMS) ages demonstrated that the core spanned the period from the Last Glacial Maximum (LGM) to the Holocene (20-12 thousand years ago (kya)). Results derived from carbon and oxygen isotopes provide insight into the paleoclimate of the Southern Levant. The period from 20-14.6 kya was dry and cool, with little organic matter being washed into the Dead Sea Basin. This interpretation is based on higher isotopic values ($\delta^{13}C$ values as high as 1.57) than are found in the modern Jordan River, which has $\delta^{13}C$ values of –7.2. During the interval from 14.2-12.5 kya, values for $\delta^{13}C$ and $\delta^{18}O$ were much more dilute, with $\delta^{13}C$ values as low as –14. This dilution demonstrates increased precipitation and/or flooding events that washed organic matter into the basin. The results of this study agree with other studies based on paleolake levels, pollen levels and paleoclimate studies from the Dead Sea Basin.

Archaeology and Environment of the Dead Sea Plain: preliminary results of the second season of investigations by the joint La Trobe University/ Arizona State University Project.

Phillip C. Edwards, Steven E. Falconer, Patricia L. Fall, Ilya Berelov, John Czarzasty, Christopher Day, John Meadows, **Cathryn Meegan,** *Ghattas Sayej,* **Thomas K.** *Swoveland and Michael Westaway*

Introduction

The 'Archaeology and Environment of the Dead Sea Plain' project, directed by Phillip Edwards, Steven Falconer and Patricia Fall, **conducted** its second joint field seasons at Zahrat adh-Dhra' in **January and** February 2001. The Zahrat adh-Dhra' region is located near the south-eastern corner of the Dead Sea, between Mazra' village to the west and the Jordan Valley margin to the east, on the low-lying and hyper-arid Dead Sea Plain (Fig.1). The project is currently investigating the cultural and natural history of the Dead Sea Plain **from the latest Pleistocene** through the Holocene, by combining geomorphological and palaeoenvironmental studies with archaeological investigations of sites representing two of the region's most significant eras of prehistoric agricultural intensification; namely the Pre-Pottery Neolithic A (PPNA) and Middle Bronze Age (Edwards *et al.* 2001). The earlier of the two periods is represented by the site of Zahrat adh-Dhra' 2 (ZAD 2), dating to 9,600 – 9,300 b.p. (9,100-8,550 calibrated years BC); and the second by Zahrat adh-Dhra' 1 (ZAD 1), an unusual Middle Bronze Age village (*ca.* **2000-1600** BC) situated only 200 meters from ZAD 2.

This report begins with a synopsis of the geoarchaeological survey (by Christopher Day) begun in order to provide palaeolandscape contexts for both ZAD 1 and ZAD 2 and the palaeoenvironmental core data. It continues with an account of the ongoing **AMS, isotope, varve, and palynological analyses of sediment cores** obtained from the Lisan Peninsula in **2000** (Patricia Fall and Tom Swoveland), proceeds to a description of the second season of excavations of ZAD 2 (Phillip Edwards) and the comprehensive surface architectural survey of ZAD 1 (Steven Falconer and John Czarzasty) and includes progress reports on the analysis of excavated materials: the flaked and ground-stone lithics (Ghattas Sayej), plant macrofossils (John Meadows) and human bones (Michael Westaway) from ZAD 2; and the pottery (Steven Falconer and Ilya Berelov) **and plant macrofossils (Cathryn Meegan) from ZAD 1.**

Christopher Day's geoarchaeological work concentrated on the major Zahrat adh-Dhra' region, situated between the Kerak Road to the east and the roughly triangular area bordered to the west by the merging channels of Wadi Kerak and Wadi adh-Dhra'. Surprisingly for a region with such a high archaeological profile, this particular area, which we have also christened the 'ZAD Triangle', appears to have never been made the subject of any previous comprehensive archaeological survey.

The geoarchaeology of Zahrat adh-Dhra' – the 'ZAD Triangle'

The location of a PPNA hamlet and an MB village (ZAD 2 and ZAD 1) on the arid and dissected Zahrat adh-Dhra' plain represent two rare examples of settlement and agriculture in this region at critical junctures in the developmental trajectories of the Southern Levant. The evidence from two seasons of investigation implies a history of settlement and land use in a setting more benign than is suggested by the present badland and deeply incised wadis that surround both sites. The aim of geoarchaeological investigation in the ZAD Triangle was to address several local and regional questions about the nature and rate of landscape change and the adaptation to the peculiar geological setting and resources of Zahrat adh-Dhra'.

This work involved reconnaissance survey of the regional geology – currently available at only 1:50,000 scale- and interpretation of local geomorphology by which archaeological visibility and past land use might be reconstructed. During the course of this survey several new sites were recorded. The distribution and dating of these sites will greatly assist our understanding of the timing of landscape change at Zahrat adh-Dhra'. One specific and ongoing geoarchaeological issue at ZAD1 is whether two large boulder walls at the northern and southern ends of the site were natural or man-made structures. Further, a sequence of low terraces in the channel of Wadi adh-Dhra' below ZAD 1 which contain fine charcoal horizons was sampled in 2000. The prospect that this material might be a source of off-site colluvium was also investigated during the 2001 program.

Geological and geomorphological survey
A comprehensive geological survey revealed better resolution of the Dana Conglomerate (DC) and its relationship with overlying Pleistocene gravels. The lithological differences and landform development within the DC provide data about past landscapes, land use and the survival of archaeological remains. The Dana Conglomerate outcrops at Zahrat adh-Dhra' as a series of monoclines **that** dip gently to the southeast, capped by resistant silicified black cherts. Less resistant reddish and white sandstone units are exposed on the plains to the east of ZAD 1 and ZAD 2 but these are blanketed by Pleistocene gravels which thicken to the south beneath ZAD 1. Indurated sandstone beds some 1-metre thick outcrop near ZAD 2, above which the softer sandstones form a dissected badland terrain. Wadi adh-Dhra' is a permanent stream and has incised some 20-30 metres below the level of neighbouring smaller wadis, exposing 60-metre sequences of the conglomerate and sandstone units within the DC. Dissection also appears to be controlled by the Pleistocene gravels – the product of earlier outwash fan deposition from Wadi adh-Dhra' at the Jordan Valley edge - which form a cap above the softer sandstones. According to the geological handbook for the region (Khalil 1992), the Dhra' Plain is also shaped by several faults, one of which is continuous through Wadi adh-Dhra'. The presence of a small doleritic basalt dyke some 300 metres upslope from ZAD 1 and ZAD 2 provides evidence that tectonic and volcanic activity – which is associated with this fault further east – continues through Zahrat adh-Dhra'.

The boulder fields at ZAD 1
Investigation of the substantial alignments of boulders at both the southeast and northwest ends of ZAD 1 revealed that they were composed of silicified limestone, commonly sub-rounded, with dissolution pitting and honeycomb weathering. Some large boulders have become fragmented due to weathering. The issue about whether this alignment of boulders is a natural or man-made feature remained unresolved

2

during the first season. The fact that no similar arrangement of large boulders existed anywhere else of the plain seemed to suggest that the boulders were transported from elsewhere. Excavation in and around the boulders however (Falconer, in Edwards et al. 2001), seemed to indicate that they were set firmly within undisturbed natural gravels, suggesting a natural feature. Survey during 2001 however noted a similar wall of similar dimensions on the north bank of Wadi Kerak about 1 kilometre away, providing a local analogue for such a construction.

During geological mapping the presence of large limestone boulders (erratics) was noted scattered throughout the valleys in the mid and upper parts of the hills immediately behind ZAD 1 and ZAD 2. Limestone is not part of the Dana Conglomerate, hence dispelling any notions that this material outcrops in the area immediate to ZAD 1. The scatters of erratics were traced almost to the Jordan Valley edge and are the product of material breaking from the ASL (Amman Silicified Limestone) unit which outcrops in dramatic vertical sheets (flatirons) some 2 kilometres to the east of the sites.

Large fragments of ASL, mobilised during erosion or tectonic episodes, form coarse debris flows and accumulate as lag deposits at the break of slope and on the near plain. It is a preliminary suggestion that such lag deposits have been the source of large stone for both wall construction and building material. ZAD 1 appears to lie at the end of a valley within which large erratics have been confined. This is supported by the observation that the DC is a poor source of building stone, with construction activities at Zahrat adh-Dhra' instead enabled by the appropriation of plentiful scatters of limestone. The concentration of large boulders as terminal lag material could reasonably have been rearranged as a substantial wall or territorial marker.

Colluvial terraces at Wadi adh-Dhra'
The presence of multiple charcoal horizons within fine-grained sand and silty terrace deposits up to 3 metres thick on the northern side of Wadi adh-Dhra' below ZAD1 was attested during the first season. While undated, the fine lamination and cross bedding, and the succession of charcoal horizons suggested that these colluvial deposits might be a potential source **of ancient** cultural material. During the second season, charcoal within a colluvial section below ZAD 1 was sampled for dating. The exposure at this sampling site was extended to a depth of 215 centimetres, revealing further thin charcoal horizons and silty material above basal cobbles. During final preparation of this section for description a piece of black plastic was found embedded within the cobbles at about 200 centimetres **below the modern terrace surface**. The deposition of over 2 metres of alluvium or colluvium in recent times provides a clear example of the rapid rate of aggradation of sediment and complexity of deposition within these arid-land wadis. Up to four phases of deposition were recorded in the exposure with fine organic silty material (local colluvium) and continuous thin charcoal horizons separated by thick sequences of fine sandy silt (alluvium). The latter commonly contained evidence of cross bedding and fine lamination.

Landscape Archaeology
The region of Zahrat adh-Dhra' between Wadi Kerak, Wadi adh-Dhra' and the Jordan Valley margin (the 'ZAD Triangle') appears to have remained unsurveyed in any systematic fashion. Reference to various past archaeological surveys in the region

3

appear for the most part to have focused in and around Bab adh-Dhra' and further south (Rast and Schaub 1981), or to the north of Wadi Kerak (Worschech 1985) or to the west (McConaughy 1981). However survey reports do not appear to have reviewed the ridge under discussion. During the second season four new major archaeological sites were discovered in the course of the geological mapping program:

a) a substantial limestone wall (mentioned above) constructed from large boulders some 100 metres above a parallel lower wall of smaller boulders on the northern bank of Wadi Kerak, about 1 kilometre north of ZAD 1. Several curvilinear walls and internal structures were noted with a scatter of possibly Bronze Age Pottery throughout, but most prominent on a hillock above the upper wall.

b) a rectangular enclosure about 80 metres by 150 metres, bounded by a loose and sparse scatter of cobbles and chert fragments on a gentle plain south of Wadi Kerak and north of black chert hills in the northern part of Zahrat adh-Dhra'.

c) a square enclosure, about 80 metres by 80 metres, located 300 metres to the northeast of ZAD 2 on a flat plain. Some 10-15 small stone features (3.5 x1.5 m.) are aligned around the western and southern perimeters.

d) A landscape of curvilinear walls, straight walls, square structures, round walled enclosures (up to 26 metres in diameter) and 10 to15 twin-chambered burial cairns extends over terrain rising from Zahrat adh-Dhra' east of the black chert range, about 500m northeast of ZAD 2. Pottery scatters suggest a Chalcolithic to Early Bronze date range.

The accurate survey and dating of the multi-period settlement of the region immediately surrounding ZAD 1 and 2 will greatly enhance the understanding of the land use history and chronology of landscape change of the Dhra Plain. The relationship and date of these other features to local landforms, particularly the evidence of truncation, will provide better resolution to models of the timing and phases of erosion in and around ZAD 1 and 2.

Future Questions

(a) The Dead Sea level fluctuations modelled by Donahue (1985), and Frumkin and colleagues (1994), is yet to be fully reconciled with the archaeological timing of erosion through ZAD 1 and 2. Future work will involve a collation of **previous interpretations** of climatic and Dead Sea level change with **new palaeoenvironmental data** from the 2000 **coring operation** and the 2001 geomorphological survey.

(b) Air photographic interpretation of the region will greatly assist geological and geomorphic interpretation.

(c) The sequence and distribution of settlement and land use on the Dhra' Plain has yet to be mapped and dated. This has considerable potential for constructing a chronology of landscape change at ZAD 1 and 2.

4

Future work will include a regional survey of these features at Zahrat adh-Dhra'.

The results of the 2001 geo-archaeological survey have placed the PPNA and MB sites in a better regional geological and geomorphological context. On a gentle plain at the fringe of the Jordan Valley both settlements benefited from the perennial spring-fed Wadi adh-Dhra', and abundant sources of flint and natural tumbles of building stone concentrated in break of slope lag deposits for opportunistic use as town walls and building stone. The Dana Conglomerate and structural features have produced a landscape of differential weathering shaped by phases of incision, the chronology of which will be better understood by a regional examination of both environmental data and wider settlement distribution.

(CD)

Palaeoenvironmental investigations on the Lisan Peninsula, Dead Sea

An important aspect of the joint La Trobe/ Arizona State University Archaeology and Environment of the Dead Sea Plain Project is to explain the sporadic settlement history on the Dead Sea Plain and the interaction of these human settlements with their past environmental landscape. Both ZAD 1 and ZAD 2 at approximately 200 m below mean sea level lie along the ancient Pleistocene shoreline of Lake Lisan (70,000-11,000 years BP). As part of our ongoing investigations to interpret the paleoclimate and past environments of this hyperarid region, we collected eight sediment cores from four localities on the northwestern end of the Lisan Peninsula in January and February 2000 **(Fig. 1)**. Four of the cores (Dead Sea Cores 1-3 and Lisan Core 3) were collected with a hand-operated, piston corer (a 5cm diameter Livinston corer). The four deepest cores (Lisan 1, 2, 4, and 6) and the top 5m of Lisan Core 3 were collected with a truck-mounted, rotary drill rig operated by the Natural Resources Authority, Hashemite Kingdom of Jordan. The sediments are composed of up to 30 meters of laminated carbonate and detrital deposits. Eleven AMS ages reveal that the uppermost 18 meters span approximately the past 20,000 yr B.P. (uncalibrated radiocarbon years before present) **(Table 1)**. Carbon and oxygen isotope analyses of carbonate layers from varved sediments show changes in lake chemistry and hydrology of Pleistocene Lake Lisan (Swoveland 2001). Our focus for this report is based on Lisan Core 3 (691-1225 cm depth) that covers the latest Pleistocene interval, from 20,000 to 12,000 years ago.

Lisan Core 3 was collected near the foreshore of the Dead Sea on the Lisan Peninsula about one meter above the modern water surface that lies 404 m below sea level. Lisan Core 3 was chosen for analysis because it represents the least distorted (due to recovery by a piston corer) and most continuously laminated sediments that cover the latest Pleistocene. The top 5 m of Lisan Core 3 were recovered with the mechanized rotary drill rig in order to penetrate the uppermost halite and dense aragonite layers. Sediments below this depth were recovered with the hand-operated piston corer. A maximum depth of 1225 cm was reached with the Livingston corer. After being shipped in wooden core boxes to the Paleoecology Laboratory in the Geography Department at ASU, Lisan Core 3 was sectioned lengthwise to observe the depositional varves. Each core section was photographed with a high-resolution digital camera in

15 cm long overlapping images to produce an electronic gallery image for the entire core (see **Fig. 1**).

Lisan Core 3 is comprised of laminated sediments consisting of alternating white carbonate and dark grey-green detrital laminae (**Fig. 2**). Three wood macrofossils embedded in the laminae show that Lisan Core 3 spans the period from 20,000 to 12,000 yr B.P. (see **Table 1**). The white carbonate layers in the core were sampled approximately every 15 cm for mineral and isotope analyses. X-ray diffraction (XRD) was used to determine the carbonate mineral phase throughout the core. XRD showed that the white layers were comprised mainly of aragonite, with trace amounts of gypsum, anhydrite, calcite, and salts. Carbon and oxygen isotopes were analysed from 24 individual aragonite laminae. $\delta^{13}C$ data are presented as parts per thousand ($^o/_{oo}$) relative to the PDB (Peedee Belemnite) Standard. $\delta^{18}O$ data, presented as parts per thousand ($^o/_{oo}$), were converted from PDB by ASU's Department of Geological Sciences Stable Isotope Lab, and are expressed relative to Standard Mean Ocean Water (SMOW).

Paleoclimatic Interpretation Based on Lisan Core 3

Carbon isotopes demonstrate variability in carbon dilution and enrichment in the Dead Sea and are used as proxies for precipitation and/or fluvial run-off to the basin. $\delta^{13}C/^{12}C$ ratios with higher ^{13}C values (-7.2 to 1.8 PDB) than the modern Jordan River (-7.2 PDB) (Stiller and Magaritz 1974) are interpreted as enriched. Dilution values vary from −14.2 to −7.2 PDB. Carbon isotopes from Lisan Core 3 show considerable enrichment for the period between 20,000 and 14,500 yr B.P., as would be expected for a hypersaline lake (**Fig. 3**). Samples with ^{13}C values more dilute than the modern Jordan River are found after 14,000 yr B.P. These dilution events are interpreted to represent the influx of organic material into Lake Lisan following an influx of water from runoff, flooding, and glacial melt water from the upper watershed of the Jordan River (the mountains of Lebanon).

Oxygen isotopes are used to provide relative temperature values. Enrichment and dilution of ^{18}O are interpreted using Jordan River water as a modern analog. Katz *et al.* (1977) reported an average ^{18}O value for the Jordan River of -2.9 SMOW (-7.2 PDB). ^{18}O for Lisan Core 3 shows the same enrichment and dilution seen in the ^{13}C data (see **Fig. 3**). Between 20,000 and 14,500 yr B.P. the water of Lake Lisan is enriched in ^{18}O. Although absolute temperature values for the Dead Sea could not be assigned, this section of the core is interpreted to represent a relatively cold, stable period (**Fig. 4**). Based on dilution of ^{18}O starting about 14,500 yr B.P. the temperature of the Dead Sea rose dramatically. More extreme temperature fluctuations are interpreted for the period from 14,500 and 12,300 yr B.P.

Carbon and oxygen isotopes from Lisan Core 3 reveal that the late glacial climate of the Dead Sea region was relatively cold and dry with very little organic matter washed into Lake Lisan. This cool dry interval ended about 14,500 years ago when precipitation and runoff into the lake basin increased greatly. This interpretation supports the recent study of stratigraphic sections in the Dead Sea area by Abed and Yaghan (2000) that hypothesizes that the climate during the late glacial maximum (LGM) was cool and dry. No evidence for a pluvial climate during the period from 20,000 to 14,200 years ago, as suggested by Neev and Emery (1995), is seen in the Lisan Core 3 isotope data.

The cold and dry period identified in Lisan Core 3 between 20,000 and 14,500 years ago coincides with the Early Epipalaeolithic Period (20,000 to 15,000 yr B.P.) when the landscape was dominated by open steppe vegetation (Baruch and Bottema 1999) with Mediterranean forest refugia along wadis of the northern Jordan Rift Valley (Edwards 2001). During the Middle Epipalaeolithic (15,000 to 13,000 yr B.P.) locally moist environments continue along the Jordan Valley (Edwards 2001). Our results agree with palynological studies from the Huleh Basin, in the upper elevation watershed of the Dead Sea, that show that deciduous oak forests expanded between 14,500 and 12,500 years ago in response to a warmer and wetter climate (Baruch and Bottema 1999). After about 12,500 years ago the climate of the region deteriorated, with dry conditions returning in the southern Levant (Baruch and Bottema 1999; Yasuda *et al.* 2001) as forests became more restricted and steppe lands expanded. Stream incision due to a lowering of base level began in the Late Epipalaeolithic (12,000 to 11,000 yr B.P.) when settlement sizes increased (Edwards 2001).

Ongoing AMS, isotope, varve and palynological analyses of both the Pleistocene and Holocene portions of the cores from the Lisan Peninsula will allow us to illuminate human interaction within the context of the paleoenvironmental landscape of the Dead Sea Plain and the greater Jordan Rift Valley.

(PLF and TKS)

A second season of excavations at the PPNA site of Zahrat adh-Dhra' 2 (ZAD 2)

La Trobe University carried out a second season of excavations at ZAD 2 from January to February, 2001. The first season in late 1999 demonstrated ZAD 2 to be a small mound about two metres thick and 2,000 square metres in area. During that period, portions of three structures (Structures 1, 2 and 3) were excavated. Charcoal samples from **successive** phases of occupation in Structure 3 yielded three radiocarbon determinations of 9,490 ± 50 b.p. (OZE 605); 9,440 ± 50 b.p. (OZE 606) and 9,470 ± 50 b.p. (OZE 607) indicative of a short-lived site.

The 2001 program succeeded in excavating Structures 1, 2 and 3 through to the underlying natural sediments; excavating a larger area of deposits in Structure 2, excavating a secondary burial in Squares I-J 25, and beginning the excavation of Structure 4 in the northern part of the site (Figs 2-3). Several new radiocarbon **samples also were obtained.**

Structure 1 (Square E28)
Structure 1 is a small, round stone hut located on the western edge of the settlement (Fig. 4). In the first season, a series of interleaved, red and dark grey deposits (Loci 1-18), which appeared to represent refuse tip lines, were excavated in its Square E 28 (Fig. 6). This sondage was continued in the second season (Loci 19-26), demonstrating a gradual decrease of artefact density with depth, until natural Dana Conglomerate Formation sediments (Locus 24) were encountered at 1.20 metres below the surface. While no artefacts were found in the DC, the remains of a child's skull were found dug into a small pit (Locus 25), some 10 centimetres deep into the natural layers (Fig. 6, 9). The skull survived mainly as an endocast of sediment

supplemented by a partial covering of thin cranial bone fragments, surmounted by a little molded dome of mud. Underneath this arrangement a number of loose, deciduous teeth were discovered.

Depth of deposits in Structure 2 (Squares K 22 – L 23)
The first season excavations showed Structure 2 to be associated with a plastered floor (Locus 3.1) and an interior hearth (F.4) set with stones and plaster in Squares K 22 – L 23. Excavations were extended here during 2001, revealing three additional superimposed floors between Locus 3.1 and the natural some 60 centimetres below (Fig. 7). The next floor (Locus 4.1) encountered below Locus 3.1 was varied in character (Fig. 10), changing from a hard plastered surface in the south to softer brown sediment in the north. The two regions were divided by a low, single coursed wall of stone, mudbricks and mortar (F. 3). The hearth (F. 4), which was plastered over by Floor 3.1, proved to be founded on an underlying third floor (Locus 5.1). In the course of excavations beneath this locus a new feature (F. 2) emerged: a U-shaped stone platform abutting the main wall (F. 1). This was probably an earlier hearth and it rested on the fourth floor (Locus 6.1). The bottom of the wall (F. 1) was associated with this lowest fourth floor and revealed a six-coursed, double-rowed, well-mortared limestone wall standing to a height of 0.8 metres. No foundation trench was discovered, although hard mortar and a number of stones associated with the base of the wall may have functioned to stabilize it. Finally, excavations in K 22 reached the natural Dana Conglomerate at about 90 centimetres below surface sediments. This (Locus 7.1) consisted of a shelf of hardened, lithified Dana sediment sloping up to the north.

Lateral extent of Structure 2
During the first season, excavations revealed that Structure 2 possessed a long curvilinear stonewall arc (Feature 1 = F. 1), which curved from the northwest in Square J 22 to the southeast in Square K 24. In the second season this wall was further traced to reveal an entire walled enclosure (Figs 2, 11). The southern and eastern parts of the excavations proceeded in 18 squares (L 26 – S 22). In Squares L 26 – O, the structure curved sharply around to the east. In this sector, where the wall was dug to the uppermost floor (Locus 5), the six-coursed wall reached a height of 80 centimetres (Figs 9-10). A single-coursed stone wall (F. 6) was found running from F. 1 to the south, in Squares N/O –28, apparently connected to it at a later date (Fig. 11). Squares O 26 – S 22 saw F. 1 straightening as it ran towards the northeast.

In the north, Feature 1 also ran sharply to the east through Squares K 20 to O 20. Square O 20 touched on the edge of another human burial, inside the fill of Structure 2, which was left unexcavated. An old clandestine excavation pit precluded clarification of any further continuation of the wall to the northeast, but excavations in Square P19 demonstrated no linkage of the northern and eastern parts of the curvilinear wall, indicating the placement of a door or opening in this area. This is considered especially likely as the wall-section in Squares Q/R 22 stops abruptly. It appeared to be finished to a squared face rather than destroyed.

In summary, Structure 2 has proved to be a most unusual design for the PPNA. Its shape is difficult to describe, but appears as a constricted 'teardrop'-shaped structure opening to the east, with its major axes measuring some 7 metres in length (Fig. 11). A further surprise is that the eastern wall of Structure 2 appears to swing round to the

8

southeast to continue as Structure 3, though this awaits clarification by further excavation.

The secondary burial in Squares I- J-K 25
A second wall (F. 2) abutted F. 1 in Square J 22 and curved away in the opposite direction (to the southwest). In 1999, a small cairn of stones (F. 3) was discovered, positioned in the interstices between the two walls near the south baulk of Square J 24, and this overlay some large fragments of a human cranium. Further excavation showed that F.3 marked the northern end of a complete human skull which emerged in the baulk. This burial (F. 5) was excavated in 2001 (see report by MW below).

No burial pit was visible at any stage of the excavations. The bones were embedded in dark and friable ashy deposits throughout, and deposited in fill on or near to the uppermost floor between the two structures. Several large rocks based around the skull form a continuation of the small cairn (F. 3) first discovered in Square J24. The burial continued west of I25, in the direction of a clandestine excavation pit. Many artefacts were recovered from the shallow deposits, the most notable being a small stone phallic figurine (Fig. 13).

Structure 3 (U-V 22)
In the first season, two squares (U-V 22) were positioned at the summit of the site in order to investigate the deepest deposits of the site. In Locus 2.1, about 40 centimetres below the surface, a hearth (F. 3) rich in charcoal was found associated with a floor. This capped the underlying Structure 3 which consisted of a curvilinear wall stepped down to the north, curving east to west from Square V 22 to U 22, with the interior floored surface some 25 centimetres below the exterior one. Excavations in the second season were designed to determine whether Structure 3 overlay an earlier structure or not, and in any case to excavate to natural sediments.

Only two thin layers (Loci 7.3 and 7.4), including the basal floor of Structure 3 (Locus 7.4), had to be removed before the season's goal was achieved (Fig. 8). Below these layers the sterile Dana sediment (Locus 7.5) was encountered and dug down 45 centimetres without further architectural finds appearing. Like Structure 2, the base of the main wall (F. 1) was not set into a foundation trench, but was laid on a mortar base. The Structure 3 wall was dismantled in Square V22, showing that the stones were set into copious, hard mortar layers. This left a patch of exterior surfaces to be excavated from the small, triangular area in the northeast corner of V22. Two sharply defined and superimposed white plaster floors were encountered here, one associated with the external base of F. 1.

Structure 4 (Squares K11 –Q10)
Clearance of Structure 4, located in the northern part of ZAD 2, was initiated in the second season. Excavation in thirteen squares metres tracked a large curvilinear wall segment (F. 1) running in a northwest to southeast direction (Figs 5, 12). Excavations in Square P 10-11 and Q 10 indicated the wall to be but one course thick, with a maximum height of 0.25 metres and width ranging from 0.55 – 0.68 meters, sitting on a thin layer of small pebbles and rocks. Hence, subsequent excavation was directed laterally wherever this horizon was encountered. Numerous stones were missing from the wall in Squares O11 and O12, and a large amount of tumble was scattered on its

southern, exterior side. In Squares L-O 11 on the interior of Structure 4, the single wall course was associated with a cobblestone floor composed of pebbles and small stones set into a coarse, grayish plaster. All of these strands of evidence support the conclusion that Structure 4 is much less well preserved than its more southerly counterparts, and this is attributable to its position near the edge of the mound where deposits are thinner.

Summary of ZAD 2 architecture
The 2001 excavations confirmed the evidence previously obtained in 1999, in demonstrating that ZAD 2 was a short-lived settlement or round and teardrop-shaped stone huts, containing only one major construction phase. Where we have excavated the structures appear to be individual structures whose external walls adjoin other structures. Despite the tightly clustered series of radiocarbon dates, it is not necessarily the case that all of the structures were planned and built at one time. Rather, there is some evidence in the way that Structure 2 seems to 'onlap' Structure 3, and the later exterior walls abutting Structure 2 (e.g. F. 6) to suggest that the huts were added to laterally over time. Within individual structures there are multiple floor phases – up to four in the case of Structure 2. Structures 1, 2 and 3 were dug though to sterile deposits at about 1 metre below the surface, showing that the low rise of the mound (ca. 1-2 metres) is partially natural.

In some cases walls of one structure continue on to form part of another. The architecture is notable for its regularity and high standard of construction, and can currently be counted as the most substantial architectural array for the PPNA period on Jordan. It is difficult to find exact parallels to ZAD 2's array of adjoining round, oval and teardrop-shaped stone huts, but it does recall another late PPNA architectural complex at Jerf al-Ahmar in northern Syria (in Phase I on the eastern mound; Stordeur 1999:140).

Various artefacts and materials from ZAD 2 in 2001
The most unusual find from the 2001 excavations was a small figurine made of an undetermined stone (Fig. 13), found in the J 25 burial (RN 010036). More malachite fragments, some facetted, a red (coral?) bead, Dentalium shells and retouched lithics, a complete basalt pestle (RN 010065) and a cuphole mortar (010069) numbered among other prominent finds.

Stratigraphy and chronology of Zahrat adh-Dhra' 2
Six additional AMS radiocarbon dates from ZAD 2 have been acquired after the second season, augmenting the three obtained from the first season (Table 1). All samples were run on small and chunky wood charcoal fragments, which are abundant in almost every excavation context throughout the site. Those **that** can be identified (pers. comm. Patricia Fall) have proved to derive from the branches and twigs of fig (*Ficus* sp.) and oak (*Quercus* sp.) trees.

In Structure 1, the date of 9,552 ± 59 b.p. (Wk-9455) comes from the lowermost occupation layer of Square E 28, (Locus 22.3) and overlies the infant skull remains dug into the Dana Conglomerate. A date of 9,635 ± 59 b.p. (Wk- comes from Locus 20.1, some 15-20 centimetres higher than Locus 22.3. According to the method of Gillespie (1982), which is based on that of Ward and Wilson (1978), the two dates are statistically indistinguishable. The calculated value of the Test statistic T is 0.520,

which is less than the tabled value of Chi-Squared (3.841) for one degree of freedom at the 0.05 level, indicating a 95 % probability that the two ages share the same true mean age.

Structure 2 yielded three superimposed AMS dates. The first is 9,323 ± 59 b.p. (Wk-9444) **that** comes from a deposit (Square L 23, Locus 3.2) underlying the uppermost floor. The next date of 9,623 ± 91 b.p. (Wk-9568) comes from the layer (Square K22, Locus 3.3) immediately underlying Wk–9444. The final date 9,603 ± 59 b.p. (Wk-9447) is from the earliest and lowest of Structure 2's four floors (Square K22, Locus 6.1). The calculated value of the Test statistic T for the means of these three determinations is 3.783, which is less than the tabled value of Chi-Squared (5.991) for two degrees of freedom at the 0.05 level, indicating a 95 % probability that the three ages share the same true mean age.

For Structure 3, a fourth date of 9,528 ± 61 b.p. (Wk-9570) can now be added to the trio obtained from the first season. Wk-9570 is from the lowermost floor of Structure 3 (Square U22, Locus 5.4). Only a thin layer (Locus 7.3) separates this date from the overlying ones of 9,440 ± 50 b.p. (OZE-606) and 9,470 ± 50 b.p. (OZE-607), both on Floor 7.2 of Square V 22, which are in turn overlaid by the date of 9,490 ± 50 b.p. (OZE-605) underlying the uppermost floor (Square V 22, Locus 3.1). The calculated value of the Test statistic T for the means of these four determinations is 1.358, which is less than the tabled value of Chi-Squared (7.815) for three degrees of freedom at the 0.05 level, indicating a 95 % probability that the four ages share the same true mean age.

Together, the suite of radiocarbon dates shows a strong degree of concordance. Indeed, T calculated for eight of the nine dates (minus the most recent one of Wk-9444, 9,323 ± 59 b.p.) is 11.605, which is less than the tabled value of Chi-Squared (14.067) for seven degrees of freedom at the 0.05 level, indicating a 95 % probability that the eight ages share the same true mean age. Only when Wk-9444 is added in does this concordance break down, giving a T-value of 21.942, which exceeds the tabled value of Chi-Squared (15.507) for eight degrees of freedom at the 0.05 level, indicating that the means of all the dates are statistically distinguishable and cannot be assumed to be derived from the same mean age.

ZAD 2 is now a well-dated Pre-Pottery Neolithic site. The single constructional phase across the site and the suite of concordant dates point to a short-lived settlement. Just a single date (9,323 ± 59 b.p.) suggests that the settlement persisted for more than about a century, and, at the outside, ZAD 2 spans the period from 9,600 to 9,300 b.p.

The implications of ZAD 2 for the transition between the PPNA and the PPNB

In view of recent uncertainties about the nature of the passage from the PPNA to the PPNB in Jordan (Kuijt 1997, Rollefson 2001), the dating of PPNA ZAD 2 to 9,600 – 9,300 b.p is a most extraordinary outcome, because the site slots neatly into the time frame of 9,600 – 9,200 b.p. proposed for the 'Early PPNB' (EPPNB) period (Rollefson 1989, 2001). The EPPNB in Jordan was advanced on the basis of such a phase in Syria, as attested at Tell Aswad (De Contenson 1989). However, the putative EPPNB in Jordan has hitherto entirely lacked any dated or excavated archaeological sites to fill it. Moreover, the PPNA at Jericho and Netiv Hagdud persists until 9,300 b.p., and because of these considerations and the fact that socio-cultural, architectural and economic shifts

11

towards sedentism and farming in Syria are known to precede the same transitions in the southern Levant, Kuijt (1997) has argued strongly against the EPPNB's existence in Jordan and for an extension of the PPNA in Jordan until ca. 9,300 b.p.

On the uncalibrated radiocarbon scale, ZAD 2 now provides conclusive evidence for an extension of the PPNA in the southern Levant till 9,300 b.p., and conversely, the site militates against the existence of the EPPNB in Jordan. Nonetheless, the employment of uncalibrated radiocarbon dates per sé is problematic in this regard, because uncalibrated dates do not represent true sidereal time. In particular they are problematic in the period from 9,600 to 9,400 b.p. which coincides with a marked 'flat spot' on the dencrochronological calibration curve (Edwards and Higham 2001). For example, calibration of the ZAD 2 dates (ranging *ca.* 300 years) leads to a greatly expanded calibrated time slice, from 9,250 BC to 8,330 BC, or nearly a thousand years.

In so far as the uncalibrated chronology is accepted, the extension of the Jordanian PPNA down to 9,300 b.p. is not just a matter of changing the chronological borders a little. It also highlights the transition in Jordan between the late PPNA of 9,300 b.p. and the large MPPNB settlements after 9,200 b.p. as a more acute one than we have previously realized. For the Dead Sea region, the contrast is best exemplified by the gulf between tiny ZAD 2 and the massive architectural elaboration of MPPNB (from *ca.* 9.000 b.p.) Wadi Ghuwair I (Najjar 2001). In view of the prior PPNB developments in the north, it now becomes increasingly difficult to derive the MPPNB village solely from the small late-PPNA hamlet of ZAD 2-type, and increasingly likely that strong influences from the northern Levant were introduced around 9,200 b.p., just as economic changes such as the introduction of livestock herding (Martin 2000) later were.

(PCE)

Footnotes

References

Abed, A. M. and R. Yaghan
2000   On the paleoclimate of Jordan during the last glacial maximum.
         Palaeogeography, Palaeoclimatology, Palaeoecology **160:23-33.**
Baruch, U. and S. Bottema
1999   A new pollen diagram from Lake Hula. In H. Kawagoe, G.W. Coulter,
         and A.C. Roosevelt (eds.) *Ancient Lakes: Their Cultural and Biological*
         Diversity, **pp. 75-86. Kenobi Productions:Belgium.**
De Contenson, H.
1989   L'Aswadien: un nouveau faciès du Néolithique Syrien. *Paléorient* 15/1:
        259-262.
Donahue, J.
1985   Hydrologic and topographic change during and after Early Bronze
        occupation at Bab adh-Dhra' and Numeira. In A. Hadidi (ed.*) Studies in the*
        History and Archaeology of Jordan II, pp. 131-140. Department of Amman:
        Antiquities of Jordan/ London: Routledge & Kegan Paul.
Edwards, P.C.
2001   Nine millennia by Lake Lisan: the Epipalaeolithic in the east Jordan Valley
         between 20,000 and 11,000 years ago. In ....
Edwards, P.C. and T. Higham
2001   Zahrat adh-Dhra' 2 and the Dead Sea Plain at the dawn of the Holocene. In A.
        Walmsley (ed.), *Australians uncovering ancient Jordan: fifty years of Middle*
        Eastern Archaeology, pp. 139-152. The Research Institute for Humanities and
        Social Sciences, University of Sydney: Sydney.
Edwards, P.C., S.E. Falconer, P.L. Fall, I. Berelov, C. Davies, J. Meadows,
C. Meegan, M.C. Metzger and G. J. Sayej
2001   Archaeology and Environment of the Dead Sea Plain: preliminary results of the
        first season of investigations by the joint La Trobe University/ Arizona State
        University Project. *Annual of the Department of Antiquities of Jordan* 45
        (in press).
Frumkin, A., I. Carmi, I, Zak and M. Margaritz
1994   Middle Holocene environmental change determined from the salt caves of
        Mount Sedom, Israel. In O. Bar-Yosef and R.S. Kra (eds) *Late Quaternary*
        chronology and Paleoclimates of the Eastern Mediterranean, pp. 315-332.
        Tucson: RADIOCARBON, University of Arizona.
Katz, A., Y. Kolodny, and A. Nissenbaum
1977   The geochemical evolution of the Pleistocene Lake Lisan-Dead Sea system.
         Geochimica et Cosmochimica Acta **41:1609-1626.**
Khalil, B.
1992   *The Geology of the ar-Rabba area. Map Sheet no. 3152 IV.* Amman: Bulletin 22,
        Geology Mapping Division, Geology Directorate. Ministry of Energy and
        Mineral Resources / Natural Resources authority, Hashemite Kingdom of
        Jordan.
Kuijt, I.
1997   Trying to fit round houses into square holes: re-examining the timing of the
        South-Central Levantine Pre-Pottery Neolithic A and Pre-Pottery Neolithic B
        cultural transition. In. Gebel, H.G. K., Z. Kafafi and G. O. Rollefson (eds),

The Prehistory of Jordan, II. Perspectives from 1997, pp.193-202, *ex oriente*, Berlin.

Martin, L. A.
2000   Mammal remains from the eastern Jordanian Neolithic, and the nature of caprine herding in the steppe, *Paléorient* 25/2: 87-104.

McConaughy, M.A.
1981   A preliminary report on the Bab edh-Dhra site survey. In W.E. Rast and R.T. Schaub (eds) *The Southeastern Dead Sea Plain Expedition: an interim report of the 1977 season*, pp. 187-190. Cambridge, M.A.: American Schools of Oriental Research.

Najjar, M.
2001   Towards a commonly accepted chronological framework of the Pre-Pottery Neolithic B Period in Jordan. In *Studies in the History and Archaeology of Jordan* VII, pp. 101-105. Department of Antiquities of Jordan, Amman.

Neev, D. and K.O. Emery
1995   *The Destruction of Sodom, Gomorrah, and Jericho: Geological, Climatological, and Archaeological Background.* Oxford: Oxford University Press.

Rast, W.E. and R.T. Schaub (eds)
1981   *The Southeastern Dead Sea Plain Expedition: an interim report of the 1977 season*. Cambridge, M.A.: American Schools of Oriental Research.

Rollefson, G.
1989   The late Aceramic Neolithic of the Levant: a synthesis. *Paléorient* 15/1: 168-173.

Rollefson, G.
2001   Jordan in the Sixth and Seventh Millennia BC. In *Studies in the History and Archaeology of Jordan* VII, pp. 95-100. Department of Antiquities of Jordan, Amman.

Stiller, M. and M. Magaritz
1974   Carbon-13 enriched carbonate in interstitial waters of Lake Kinneret sediments. *Limnology and Oceanography* 19(5): 849-853.

Stordeur, D.
1999   Organisation de l'espace construit et organisation sociale dans le Néolithique de Jerf el Ahmar (Syrie, X^e – IXe millénaire av. J.-C.). In F. Braemer, S. Cleuziou and A. Coudart (eds) *Habitat et société*, pp. 131-149. XIXe Rencontres Internationales d'Archéologie et d'Histoire d'Antibes. Editions APDCA, Antibes.

Swoveland, T. K.
2001   The paleoclimate of the Dead Sea basin from the Last Glacial Maximum to the Holocene. M.A. Thesis. Arizona State University:Tempe.

Worschech, U.F. Ch.
1985   *Northwest Ard al-Kerak 1983 and 1984: a preliminary report.* München: Beihefte 2. Biblische Notizen.

Yasuda, Y., H. Kitagawa, and T. Nakagawa
2001   The earliest record of major anthropogenic deforestation in the Ghab Valley, northwest Syria: a palynological study. *Quaternary International* 73/74: 127-136.

List of Figures

PLF and TKS Figure 1-4 –Phil you can renumber these (also in the text).

Table 1. Radiocarbon age determinations from ZAD 2

Provenance	Date (uncal. b.p.)	Laboratory Code	Calibrated date (95.4% probability) OxCal.version 3.4
Structure 1 Sq. E 28, Loc. 20.1	9,635 ± 59	Wk-9633	9,230 – 8,790 BC
Structure 1 Sq. E 28, Loc. 22.3	9,552 ± 59	Wk-9445	9,250 – 8,650 BC
Structure 2, Sq. K 22, Loc. 6.1	9,603 ± 59	Wk-9447	9,220 – 8,790 BC
Structure 2, Sq. K 22, Loc. 3.3	9,623 ± 91	Wk-9568	9,240 – 8,740 BC
Structure 2, Sq. L 23, Loc. 3.2	9,323 ± 59	Wk-9444	8,750 – 8,330 BC
Structure 3, Sq. U 22, Loc.5.4	9,528 ± 61	Wk-9570	9,200 – 8,600 BC
Structure 3, Sq. V 22, Loc. 3.1	9,490 ± 50	OZE 605	9,150 – 8,650 BC
Structure 3, Sq. V 22, Loc. 7.2	9,440 ± 50	OZE 606	9,150 – 8,550 BC
Structure 3, Sq. V 22, Loc. 7.2	9,470 ± 50	OZE 607	9,150 – 8,600 BC

Table 1. AMS age determinations from Dead Sea and Lisan Cores

Core	Depth (cm)	Age (uncalibrated yr B.P.)	Laboratory Number	Calibrated Age (95% probability) Stuiver *et al.* 1998
Dead Sea 3	8.5	1440 ± 40	Beta-160106	AD 550-660
Dead Sea 3	26	1590 ± 40	Beta-160107	AD 400-560
Dead Sea 3	45	1690 ± 40	Beta-153581	AD 250-430
Dead Sea 3	108	1820 ± 40	Beta-153582	AD 100-260 and AD 290-320
Dead Sea 2	361	7030 ± 50	Beta-155306	BC 6000-5790
Dead Sea 2	512	5020 ± 50	Beta-155307	BC 3960-3680
Lisan 2	1461	15,190 ± 50	Beta-156767	BC 16,510-15,850
Lisan 2	1673	18,690 ± 60	Beta-156768	BC 20,730-19,770
Lisan 3	698	12,460 ± 40	Beta-153583	BC 13,490-12,220
Lisan 3	1067	17,990 ± 60	Beta-155308	BC 19,900-18,970
Lisan 3	1186	19,020 ± 70	Beta-156766	BC 21,150-20,120